

Models of Recruitment and Rate Coding Organization in Motor-Unit Pools

ANDREW J. FUGLEVAND, DAVID A. WINTER, AND AFTAB E. PATLA
Department of Kinesiology, University of Waterloo, Waterloo, Ontario N2L 3G1, Canada

SUMMARY AND CONCLUSIONS

1. Isometric muscle force and the surface electromyogram (EMG) were simulated from a model that predicted recruitment and firing times in a pool of 120 motor units under different levels of excitatory drive. The EMG-force relationships that emerged from simulations using various schedules of recruitment and rate coding were compared with those observed experimentally to determine which of the modeled schemes were plausible representations of the actual organization in motor-unit pools.

2. The model was comprised of three elements: a motoneuron model, a motor-unit force model, and a model of the surface EMG. Input to the neuron model was an excitatory drive function representing the net synaptic input to motoneurons during voluntary muscle contractions. Recruitment thresholds were assigned such that many motoneurons had low thresholds and relatively few neurons had high thresholds. Motoneuron firing rate increased as a linear function of excitatory drive between recruitment threshold and peak firing rate levels. The sequence of discharge times for each motoneuron was simulated as a random renewal process.

3. Motor-unit twitch force was estimated as an impulse response of a critically damped, second-order system. Twitch amplitudes were assigned according to rank in the recruitment order, and twitch contraction times were inversely related to twitch amplitude. Nonlinear force-firing rate behavior was simulated by varying motor-unit force gain as a function of the instantaneous firing rate and the contraction time of the unit. The total force exerted by the muscle was computed as the sum of the motor-unit forces.

4. Motor-unit action potentials were simulated on the basis of estimates of the number and location of motor-unit muscle fibers and the propagation velocity of the fiber action potentials. The number of fibers innervated by each unit was assumed to be directly proportional to the twitch force. The area of muscle encompassing unit fibers was proportional to the number of fibers innervated, and the location of motor-unit territories were randomly assigned within the muscle cross section. Action-potential propagation velocities were estimated from an inverse function of contraction time. The train of discharge times predicted from the motoneuron model determined the occurrence of each motor-unit action potential. The surface EMG was synthesized as the sum of all motor-unit action-potential trains.

5. Two recruitment conditions were tested: narrow (limit of recruitment <50% maximum excitation) and broad recruitment range conditions (limit of recruitment >70% maximum excitation). Three rate coding conditions were tested: 1) low-threshold units attained greater firing rates than high-threshold units, 2) all units were assigned the same peak firing rate, and 3) peak firing rates were matched for each unit to the stimulus frequency required for maximum tetanic force.

6. The relation between EMG and force was linear when recruitment operated over a broad force range, and peak firing rates were not the same for all units. When recruitment was complete at

low force levels (<57% maximum) the EMG-force relation, in all cases, was nonlinear and unlike that observed experimentally.

7. For the conditions that yielded linear EMG-force relationships, the relation between EMG and excitatory drive and between force and excitatory drive were both nonlinear. Because the shape of those nonlinear relationships were similar, when EMG was plotted as a function of force, a linear relation resulted.

8. When recruitment operated over a broad range and the peak firing rates were similar for all motor units, the EMG-force relation exhibited a slightly parabolic shape. As excitatory drive increased and the mean firing rates of the units converged toward the same value, rhythmic bursting was evident in the EMG. The bursting was associated with an augmentation of EMG amplitude, which induced a degree of concavity on an otherwise linear EMG-force relationship.

9. Unexpectedly, the maximum force capacity of the modeled muscle was not achieved in conditions where peak firing rates were set for each unit equivalent to the stimulus rate required for maximum tetanic force. The natural variability in interspike intervals combined with nonlinear force-firing rate curves for each unit diminished force from what would have been exerted had units discharged with constant interspike intervals.

10. The relation between the twitch force of a unit and the muscle force at which the unit was recruited was linear. However, the force added by the recruitment of a new unit was not a constant fraction of the muscle force. The force contributed by newly recruited units, relative to muscle force, declined hyperbolically as muscle force increased. This occurred because low-threshold units generated a larger proportion of their maximum force capacity when discharging at the threshold rate as compared with high-threshold units.

INTRODUCTION

The mammalian nervous system has two general means by which it can vary the force exerted by skeletal muscle: one, by altering the number of motor units that are active, termed recruitment; and two, by modulating the rate of action-potential impulses driving motor units, termed rate coding. Much is known about the individual properties of motor units (Binder and Mendell 1990, Burke 1981; Stuart and Enoka 1983), and a large body of experimental work has revealed some rules underlying the behavior of motor-unit populations. Notably, motor units are recruited in an orderly sequence, from those that produce the smallest forces to those that exert the largest forces (Henneman 1979; Riek and Bawa 1992; Zajac and Faden 1985). A number of questions remain, however, as to how a population of motor units operates as an ensemble to control force. For example, during the ostensibly simple task of grading isometric force along a target trajectory, it is unclear how the

motor system is organized to deal efficiently with a number of problems, including 1) how many motor units to activate, 2) how to modulate the force of active units such that the total force, at each instant, approximates the target value, and 3) when or at what point along the force trajectory to initiate activity in each of the participating units. These issues relate to the reliance the motor system places on recruitment versus rate coding to effect a change in muscle force and how the balance between these two processes varies over the force range (Harrison 1983; Kernell 1992).

The distributions of recruitment and rate coding along the muscle force axis may depend on the functional requirements of the muscle. It has been suggested that in small muscles of the hand, where precise gradation of force is important, the excitabilities of motoneurons may be organized to recruit all motor units at relatively low force levels, and rate coding then remains the primary means of modulating force from moderate to high levels (De Luca et al. 1982; Kukulka and Clamann 1981; Milner-Brown et al. 1973c). In contrast, motoneuron excitabilities may be broadly distributed to allow recruitment to operate over most of the force range in large muscles that generate powerful contractions (De Luca et al. 1982; Kukulka and Clamann 1981).

An association between muscle function and motor-unit organization, however, has been difficult to verify experimentally because recruitment and rate coding behaviors can be monitored for only a small fraction of the motor units participating in voluntary contractions. Furthermore, it has also been difficult to examine motor-unit function beyond about one-half the possible range of muscle force. Therefore, in an attempt to quantitatively address how populations of motor units may be organized to regulate muscle force, a model was developed to predict the number of units recruited, their firing rates, the force histories in the individual motor units, and the total force exerted by the muscle under different levels of excitatory drive to a hypothetical pool of motoneurons. The two main variables that were manipulated in the simulations were 1) the range of excitatory drive over which recruitment operated and 2) the ranges of firing rate in the individual motor units. To determine whether an adopted schedule of recruitment and rate coding provided a reasonable approximation of reality, it was necessary to compare simulated results to some measurable standard. For this reason an additional dimension was included in the model, a motor-unit-based simulation of the surface-detected electromyogram (EMG).

Like muscle force, the intensity of the EMG signal is influenced by the number of motor units active and their rates of firing. The relationship between EMG and isometric force has been well documented and generally has two forms. In many muscles, such as those controlling the fingers, the observed relationship is linear (Bigland and Lippold 1954a; Woods and Bigland-Ritchie 1983). In other muscles the increase in EMG for a given change in force is augmented as force levels increase giving the whole relationship a parabolic form (Lawrence and De Luca 1983; Vredenbregt and Rau 1973; Woods and Bigland-Ritchie 1983). Differences in the force range over which recruitment operates has been postulated as the main factor

underlying the two types of EMG-force relationships (Lawrence and De Luca 1983; Solomonow et al. 1986).

In the present study, for each type of recruitment and rate coding organization tested, force and EMG signals were simulated at a number of levels of excitatory drive. A plot of EMG amplitude versus force was then constructed from the simulated results and compared with empirically derived EMG-force relationships. Simulated EMG-force relationships were like those observed experimentally only under the condition of a broad recruitment range. When narrow recruitment ranges were implemented, the simulated EMG-force relations were unlike experimental ones. These results suggested that motor-unit pools may be organized with recruitment distributed over a wide force range. A short account of this work has been presented previously (Fuglevand et al. 1989).

METHODS

The model was comprised of three elements: a motoneuron model, a model of motor-unit force, and a surface EMG model. The general constraints of the model were as follows: 1) the discharge behavior of motoneurons was predicted for steady-state or slowly varying excitation; 2) feedback to motoneurons, such as that emanating from peripheral afferents, was not an explicit feature of the model; and 3) motor-unit force was simulated for isometric conditions only. Other specific limitations and assumptions for the individual model elements are detailed in the following sections.

Motor neuron pool model

The initial segment of the motoneuron axon, which serves as the trigger zone for action-potential generation (Schwindt and Crill 1984), continually integrates excitatory and inhibitory synaptic potentials that arise from a complicated array of input sources (Henneman and Mendell 1981; Munson 1990). Many factors are known to influence how input from a presynaptic source is transformed into a postsynaptic potential change at the trigger zone. The intent of the model, however, was not to characterize the specific mechanisms that shape a neuron's response to synaptic input; rather, it was to develop a realistic simulation of the output behavior of a population of motoneurons associated with voluntary activation of muscle. A functionally based approach, similar to that recently reported by Heckman and Binder (1991), was therefore adopted in which only a few parameters needed to be defined for each motoneuron.

RECRUITMENT. Two parameters were defined for simulation of motoneuron recruitment. One parameter, termed excitatory drive (E), represented the net input seen at the trigger zone due to all synaptic sources active during voluntary muscle contraction. This parameter is closely related to effective synaptic current (Heckman and Binder 1988), which represents the component of synaptic current that reaches the soma and trigger zone. The second parameter, referred to as recruitment threshold excitation (RTE), was defined as the minimum level of excitatory drive required to initiate repetitive discharge in a motoneuron. This term is essentially equivalent to the empirically determined threshold current for repetitive discharge (Kernell and Monster 1981). Two issues addressed in simulating motoneuron recruitment were 1) the distribution of synaptic input (in terms of excitatory drive, E) across the members of the motoneuron population and 2) the relative excitabilities (in terms of recruitment threshold excitation, RTE) of the individual motoneurons.

Distribution of synaptic input. The sources of synaptic input to motoneurons diverge extensively and appear to act on a broad

segment of the pool (Fleshman et al. 1981a; Harrison and Taylor 1981; Mendell and Henneman 1971; Munson et al. 1984; Sypert et al. 1980). Although the distribution of effective synaptic current may vary from one type of input to another (Heckman and Binder 1990; Lindsay and Binder 1991), it was assumed that the sum of these inputs would provide, on average, a roughly uniform distribution across the population of motoneurons. Therefore all motoneurons were modeled to receive the same level of excitatory drive.

Relative excitabilities of motoneurons. Motoneurons are normally recruited in a fixed order (Henneman 1957; Henneman et al. 1965a,b). This orderliness is likely due, in part, to systematic differences in the excitabilities of the motoneurons. Broad variation (10- to 30-fold) in rheobase (Fleshman et al. 1981b; Gustafsson and Pinter 1984; Powers and Binder 1985; Zengel et al. 1985) and in the threshold current for repetitive discharge (Kernell and Monster 1981) has been observed among the motoneurons of a pool. The frequency distribution of motoneurons based on rheobase is skewed such that many motoneurons have low rheobase and relatively few motoneurons have high rheobase (Gustafsson and Pinter 1984; Powers and Binder 1985). Therefore the values of recruitment threshold excitation (RTE) were varied across the members of the modeled pool to give many neurons low thresholds, and relatively few motoneurons were assigned high thresholds. This type of variation was modeled as an exponential in the form

$$RTE(i) = e^{a \cdot i} \quad (1)$$

where i was an index identifying the motoneuron and a was a coefficient used to establish a range of threshold values. This was facilitated by setting $a = (\ln RR)/n$, where \ln was the natural logarithm, RR was the range of recruitment threshold values desired, and n was the total number of neurons in the modeled pool. For example, to set the range of recruitment thresholds at 30-fold in a pool of $n = 120$ motoneurons, the coefficient a was computed from $a = \ln 30/120$. Then implementing Eq. 1, the recruitment threshold of the 1st (RTE_1) and 120th (RTE_{120}) neurons would be 1.0 and 30.0, respectively, and >50% of the pool would have recruitment threshold values <6.0. The units of measure for RTE , like that for excitatory drive, were in arbitrary units.

A motoneuron, i , remained inactive as long as the excitatory drive, $E(t)$, was less than the neurons assigned recruitment threshold value. The time of the first discharge (recruitment) in the i th neuron ($t_{i,1}$) occurred when the excitatory drive first equaled or exceeded the neuron's threshold value.

RATE CODING. The repetitive discharge behavior of motoneurons was characterized by four parameters: 1) the minimum steady firing rate, 2) the excitatory drive-firing rate relationship, 3) the peak firing rate, and 4) the variability in the interspike intervals (ISIs) under steady-state excitation.

Minimum firing rate. Studies using intracellular current injection have shown an inverse relationship between the minimum firing rate of motoneurons and afterhyperpolarization (AHP) duration (Kernell 1965c). AHP duration is inversely related to motoneuron rheobase (Gustafsson and Pinter 1984), which suggests, therefore, that motoneurons with low recruitment thresholds will have lower minimum firing rates than higher threshold motoneurons. However, during voluntary muscle activity in humans, minimum firing rates are similar for all motor units in a muscle, regardless of recruitment threshold (De Luca et al. 1982; Freund et al. 1975; Milner-Brown et al. 1973c; Monster and Chan 1977; Tanji and Kato 1973). This intriguing discrepancy between current-injected and voluntarily activated motoneurons implies that factors other than intrinsic motoneuron properties may be important in regulating minimum firing rate (Brownstone 1989). In the model, once a motoneuron was recruited and if excitatory drive was

maintained at the recruitment threshold level, it discharged at the minimum firing rate (MFR). The minimum firing rate was the same for all motoneurons and assigned a value of 8 imp/s.

Excitatory drive-firing rate relationship. The relationship between the steady-state level of injected current and the firing rate of motoneurons appears to be best characterized as a single (primary range), linear function (Kernell 1965b; Schwindt and Crill 1984). The gain of the current-firing rate relationship appears to be uncorrelated with indexes related to the recruitment threshold of motoneurons (Kernell 1965a, 1979). At high levels of current, a secondary range of firing is occasionally observed in which the gain is augmented (Kernell 1965b). However, many motoneurons do not display secondary range firing (Brownstone 1989; Granit et al. 1966; Kernell 1965b, 1979), and therefore it was not included in the present model.

The firing rate of a motoneuron (FR_i) was modeled to increase linearly with increased excitatory drive above the recruitment threshold excitation (RTE_i). The gain (g_e) of the excitatory drive-firing rate relationship was assigned the same value for all motoneurons. Thus the firing rate response of a motoneuron to an excitatory drive function, $E(t)$, was modeled as

$$FR_i(t) = g_e \cdot [E(t) - RTE_i] + MFR \quad E(t) \geq RTE_i \quad (2)$$

Equation 2 was rewritten by considering the instantaneous firing rate to be the inverse of the ISI and where the ISI was the time difference between two consecutive discharges

$$\frac{1}{(t_{i,j} - t_{i,j-1})} = g_e \cdot [E(t) - RTE_i] + MFR \quad E(t) \geq RTE_i \quad (3)$$

The time of the j th discharge in motoneuron i ($t_{i,j}$), for an excitatory drive function $E(t)$, could therefore be expressed as

$$t_{i,j} = \frac{1}{g_e \cdot [E(t) - RTE_i] + MFR} + t_{i,j-1} \quad E(t) \geq RTE_i \quad (4)$$

Equation 4 was solved by substituting the value of E for incremental increases in t until an equivalence between the two sides of the equation was achieved. Repetition of this process allowed for the determination of all the discharge occurrences over the simulation period in each of the modeled motoneurons. At this stage, variability in the ISIs had not been added; the manner in which this was done is discussed in a later section.

Peak firing rates. Firing rates in motoneurons increase with increased excitatory drive up to a certain level, beyond which little change in firing rate is observed. This plateau in firing rate is seen in cat motoneurons activated with current injection (Brownstone 1989), activated by reflex pathways (Burke 1968; Cordo and Rymer 1982; Granit 1958), and during locomotion (Hoffer et al. 1987); and in human motor units during voluntary contractions (Gydkov and Kosarov 1974; Monster and Chan 1977). The peak firing rates that have been observed in human muscle during non-ballistic isometric contractions have generally ranged from 20 to 45 imp/s (Bellemare et al. 1983; Bigland-Ritchie et al. 1983, 1992; De Luca et al. 1982; Freund et al. 1975; Gydkov and Kosarov 1974; Monster and Chan 1977; Tanji and Kato 1973).

How peak firing rates are related to the recruitment thresholds of motoneurons is, at present, unresolved. The most common observation during voluntary activity has been that earlier recruited motoneurons attain higher peak firing rates than do later recruited motoneurons in cats (Hoffer et al. 1987), in monkeys (Mallah et al. 1990), and in humans (De Luca et al. 1982; Monster and Chan 1977; Tanji and Kato 1973). However, other reports suggest that when motor-unit activity is monitored over a large force range, the firing rates of high-threshold units eventually surpass that of lower threshold units (Gydkov and Kosarov 1974). Both types of firing rate organization were tested. For the first type, the peak firing rate (PFR) of a motoneuron was scaled in inverse proportion to its recruitment threshold according to

$$PFR_i = PFR_1 - PFRD \cdot \frac{RTE_i}{RTE_n} \quad (5)$$

where PFR_1 was the assigned peak firing rate of the first unit recruited, $PFRD$ was the desired difference in peak firing rates between the first and last units recruited, and RTE_i/RTE_n represented the recruitment threshold excitation of each neuron relative to that of the highest threshold neuron. Typical values assigned to PFR_1 and to $PFRD$ were 45 and 10 imp/s, respectively. For the second type of organization, peak firing rates were related to the mechanical properties of the motor unit; large force, rapid-contracting units were assigned higher peak firing rates than were small force, slow-contracting units. The specific way in which this was done is described in a later section.

ISI variability. The asynchronous arrival of unitary postsynaptic potentials from many sources gives rise to fluctuations in the motoneuron membrane potential (Calvin and Stevens 1968; Stålberg and Thiele 1973). These fluctuations about the mean trajectory of the membrane potential between successive discharges will induce a degree of variability in motoneuron ISIs under steady-state synaptic excitation. Analysis of motor-unit discharge trains has indicated that ISIs resemble a random process with a Gaussian probability distribution function (Andreassen and Rosenfalck 1980; Clamann 1969; Stålberg and Thiele 1973). In addition, the mean and standard deviation of ISI distributions are related such that the coefficient of variation (standard deviation/mean) remains relatively constant with changes in mean ISI (Andreassen and Rosenfalck 1980; Clamann 1969). ISI variability is not related to the recruitment threshold of motor units within a muscle (Nordstrom and Miles 1991) but may differ somewhat between muscles and subjects (Nordstrom et al. 1992). The coefficient of variation in ISIs for human muscles during isometric contractions generally range between 0.1 and 0.3 (Clamann 1969; Nordstrom et al. 1992; Nordstrom and Miles 1991).

To simulate the stochastic nature of motoneuron discharge, the ISIs predicted by Eq. 3 were assumed equivalent to the mean ISI (μ) in a train of discharges. The time of each discharge was then adjusted, such that for a constant excitatory drive, the ISIs were normally distributed about the predicted mean interval, μ . The Z-score represents how far a particular value deviates from the mean in a normally distributed population and is calculated as $Z = (X - \mu)/\sigma$. In the present context, X represented the value of an ISI in a train of action potentials with a standard deviation in the ISIs of σ . The Z-score expression therefore was rearranged to

$$ISI_{i,j-1} = t_{i,j} - t_{i,j-1} = \mu + \sigma \cdot Z \quad (6)$$

The coefficient of variation ($cv = \sigma/\mu$) in ISIs was assumed to remain constant. Substitution of $\mu \cdot cv$ for σ and rearranging Eq. 6 yielded

$$t_{i,j} = \mu + \mu \cdot cv \cdot Z + t_{i,j-1} \quad (7)$$

For each discharge, Z was randomly selected from a normally distributed array of Z-scores ranging from -3.9 to 3.9. The value of Z was substituted into Eq. 7 along with the assigned value of the coefficient of variation ($cv = 0.2$) and the value of μ (predicted from Eq. 3) to find the adjusted discharge time, $t_{i,j}$. This process was repeated recursively to adjust all the discharge times for a motoneuron and then performed across all active motoneurons. The discharge times between motoneurons were therefore independent of one another. The weak tendency for motoneurons to exhibit synchronous discharge during voluntary contraction (Datta and Stephens 1990) was not a feature of the present model.

Maximum excitation. Maximum excitation was functionally defined as the level of synaptic excitation seen at the trigger zone during a maximum voluntary isometric contraction. In the context of the model, this definition denoted the level of excitatory drive necessary to bring the last recruited motoneuron to its as-

signed peak firing rate. Under this definition, Eq. 2 could be rearranged to solve for maximum excitation, E_{\max} , in arbitrary excitation units as

$$E_{\max} = RTE_n + \frac{PFR_n - MFR}{g_e} \quad (8)$$

The values of excitatory drive and recruitment threshold excitation were expressed as percentages of the calculated maximum excitation.

Isometric force model for motor units

The mechanical event associated with a motoneuron discharge is a motor-unit twitch. If isometric force production in motor units is considered as a linear process (an important nonlinearity is discussed below), then the twitch can be regarded as the impulse response of the motor-unit system. The Fourier transform of the impulse response yields the frequency response of the system (Bendat and Piersol 1980). The frequency response of motor units from cat hindlimb muscles, based on Fourier transformation of the twitch, has indicated that these units are well approximated as a critically damped, second-order system (Stein et al. 1972).

The impulse response, $f(t)$, of a second-order force system with critical damping can be expressed as (Milner-Brown et al. 1973c; Winter 1979)

$$f(t) = \alpha \cdot t \cdot e^{-t/T} \quad (9)$$

where e is the natural constant and T is the rise time (contraction time) to peak force of the impulse response. The constant α is related to the peak amplitude of twitch force, P (Milner-Brown et al. 1973c) by

$$\alpha = P \cdot e/T \quad (10)$$

Substitution of Eq. 10 into Eq. 9 yields

$$f(t) = \frac{P \cdot t}{T} \cdot e^{1-(t/T)} \quad (11)$$

which was used to represent a motor-unit twitch (Fig. 1A). Equation 11 was then expressed for a pool of motor units as

$$f_i(t) = \frac{P_i \cdot t}{T_i} \cdot e^{1-(t/T_i)} \quad (12)$$

The manner by which the values of peak twitch force, P_i , and contraction time, T_i , were assigned for each motor unit is presented in the following sections.

ASSIGNMENT OF TWITCH PARAMETERS. *Twitch force.* The experimental work on force magnitudes (either maximum tetanic force or peak twitch force) of motor units in both animals and humans has been consistent with regard to three findings. First, twitch or tetanic force of motor units in a pool varies over a wide range, typically ≥ 100 -fold (Calancie and Bawa 1985; Goldberg and Derfler 1977; Jami and Petit 1977; Milner-Brown et al. 1973b; Monster and Chan 1977; Olson and Swett 1966; Riek and Bawa 1992; Stephens and Usherwood 1977; Wuerker et al. 1965; Yemm 1977). Second, the frequency distribution of motor units according to force is markedly skewed such that a large number of units produced small forces, whereas few units generate relatively large forces (McPhedran et al. 1965; Milner-Brown et al. 1973b; Monster and Chan 1977; Olson and Swett 1966; Stephens and Usherwood 1977; Thomas et al. 1990; Wuerker et al. 1965). And third, the force generated by a motor unit is related to its recruitment threshold (Calancie and Bawa 1985; Goldberg and Derfler 1977; Milner-Brown et al. 1973b; Monster and Chan 1977; Riek and Bawa 1992; Stephens and Usherwood 1977; Thomas et al. 1987; Yemm 1977; Zajac and Faden 1985).

These findings were incorporated into the model by assigning

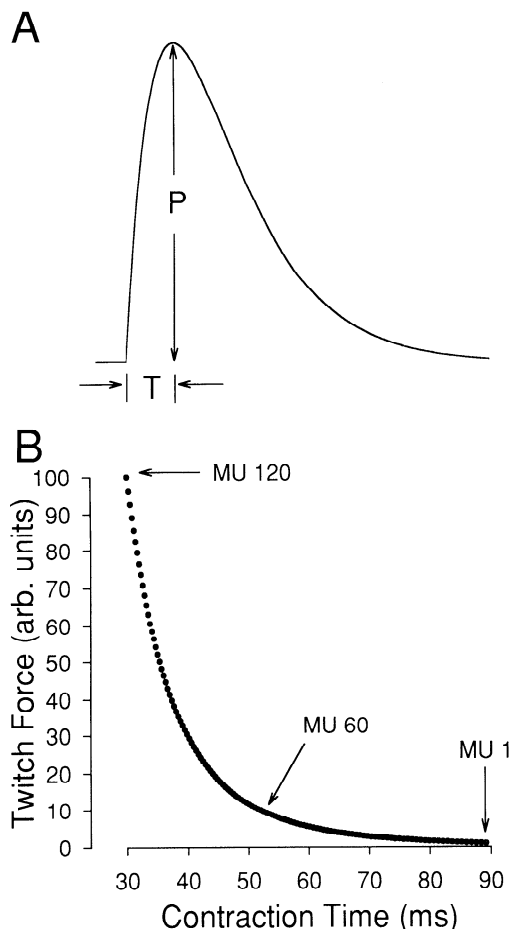


FIG. 1. A: simulated isometric force-time curve representing a motor-unit twitch. The twitch was modeled as the impulse response of a critically damped, 2nd-order system (Eq. 11). The force amplitude and contraction time of the twitch were represented by parameters P and T , respectively. B: twitch parameter assignments for entire pool of 120 motor units. Twitch forces and contraction times for each unit (\bullet) are represented as coordinate pairs on the plot. Twitch force varied over a 100-fold range with the lowest-threshold unit (MU 1) assigned the smallest force and the highest-threshold unit (MU 120) assigned the largest force. One-half the population (i.e., from MU 1 to MU 60) had twitch forces that were <10% of the largest unit's force. Contraction time varied over a 3-fold range with large force units assigned the briefest contraction times, and small force units were assigned a broad range of long-duration contraction times.

the peak twitch force (P_i) for each unit according to the following schedule

$$P(i) = e^{b \cdot i} \quad (13)$$

The form of this equation was similar to that of Eq. 1 for setting recruitment threshold values. To facilitate the assignment of a range of twitch forces, RP , the coefficient b was set as $b = -(\ln RP)/n$, where n was the number of units in the pool. The range of twitch forces (RP) used in the model was 100-fold. One unit of force was equivalent to the twitch force of the first unit recruited, and the last unit recruited had a twitch force of 100 force units.

Contraction time. The generalization that weak motor units contract slowly and strong units contract rapidly may apply directly only at the extremes of the contraction-time spectrum. Three general findings illustrate this point. First, the range of contraction times is narrow (2- to 5-fold) (Buchthal and Schmalbruch 1970; Burke 1981; Monstrey and Chan 1977; Stephens and Usherwood 1977; Thomas et al. 1987, 1990) relative to the range of twitch or tetanic forces. Second, the frequency distribution of mo-

tor units based on contraction time tends to be skewed toward brief contraction times (Fleshman et al. 1981b; Kernell et al. 1983a; McPhedran et al. 1965; Thomas et al. 1990; Wuerker et al. 1965; Young and Mayer 1981); a distribution opposite to that expected if twitch force and contractile speed were matched. And third, plots of unit force against contraction time (Burke 1981; Stephens and Usherwood 1977; Young and Mayer 1981) indicate that small force motor units have contraction times that vary over most of the range of observed values, whereas intermediate to large force units tend to be fast contracting, and the variation in contraction time among these units is small.

On the basis of these data, the relationship between twitch force (P_i) and contraction time (T_i) was approximated as an inverse power function in the form

$$T(i) = T_L \cdot \left(\frac{1}{P_i} \right)^{1/c} \quad (14)$$

The parameter T_L represented the longest duration contraction time desired for the pool. The coefficient c was determined from the expression $c = \log_{RT} RP$, where RP was the range of motor-unit twitch forces previously assigned, and RT was the range of contraction times desired. For example, if a 3-fold range in contraction time was desired for a pool of units that had a 100-fold range in twitch forces, then $c = \log_3 100 = 4.2$. If the longest duration rise time desired for the pool was 90 ms, then Eq. 14 became

$$T(i) = 90 \cdot \left(\frac{1}{P_i} \right)^{1/4.2} \quad (15)$$

A plot of twitch forces (according to Eq. 13) as a function of contraction time (according to Eq. 15) for a pool of 120 motor units is shown in Fig. 1B. Recruitment progressed from those units with long-duration contraction times and small twitch forces toward those with brief contraction times and large forces. In this scheme, 50% of the units had twitches with <10 units of force but had contraction times that covered nearly two-thirds of the range (e.g., from 52 to 90 ms).

FORCE NONLINEARITY. Studies of the frequency response of skeletal muscle have revealed a number of nonlinear properties, including a change in the gain of the nerve-muscle system as the stimulus rate was altered (Bawa and Stein 1976; Mannard and Stein 1973). The gain (output/input or force/stimulus rate) will have units of $\text{g} \cdot \text{s}/\text{imp}$ or $\text{mN} \cdot \text{s}/\text{imp}$ and can be considered as the area under the force-time curve resulting from each stimulus (Mannard and Stein 1973). The well-known sigmoid relationship between isometric force and stimulation rate (Bigland and Lippold 1954b; Rack and Westbury 1969) reflects the dependence of muscle gain on stimulus rate. The ratio of isometric force to stimulus rate (*not* the slope) at any point on the force-stimulation rate curve is equivalent to the low-frequency gain (Kernell et al. 1983b).

The specific shape of the force-stimulus rate curve depends on the contractile properties of the motor unit. The sluggish response of slow-twitch units allows the individual force impulses to summate more readily at lower stimulus rates as compared with fast-twitch units. Thus the force-stimulus rate curves for slow-twitch units rise more steeply at comparatively lower stimulus rates and attain tetanic fusion (i.e., the plateau in the sigmoid) also at lower rates than do fast-twitch units (Botterman et al. 1986; Kernell et al. 1983b; Thomas et al. 1991). If the stimulus rate, however, is normalized as a function of the time course of the twitch, the shapes of the force-stimulus rate curves are similar for most motor units (Kernell et al. 1983b). In the present model, stimulus rate ($1/ISI$) was normalized to the twitch contraction time (T_i) as T_i/ISI . The data of Burke et al. (1976) indicate that the greatest gain in motor-unit force occurs at a normalized stimulus rate of ~ 1.0 , namely, with an ISI equivalent to the twitch contraction

time. These authors also found that for normalized stimulus rates below ~ 0.4 , the gain was constant and similar in magnitude to that of an isolated twitch. The maximum observed gain (at $T_i/ISI = 1.0$) was approximately three times larger than the low stimulus rate gain.

This nonlinear force behavior was incorporated into the model by allowing the gain in motor-unit force to vary as a function of the firing rate. In each motor unit i , and for discharge j , the gain g_{ij} was derived from one of two relationships. The gain was assumed to be constant up to a normalized rate of 0.4 and to have a value equivalent to that of an individual twitch. The value of g_{ij} was considered to be the ratio of the impulse response area at any instantaneous discharge rate to the area of an isolated twitch. Thus, in the initial linear region ($0 < T_i/ISI_j \leq 0.4$), g_{ij} was assigned a value of 1.0. At normalized firing rates > 0.4 , the gain was determined from a sigmoid (S) of the form

$$S(T_i/ISI) = 1 - e^{-2(T_i/ISI)^3} \quad (16)$$

The gain was calculated as the ratio of sigmoid amplitude to the instantaneous normalized discharge rate

$$g_{ij} = \frac{S(T_i/ISI_j)}{T_i/ISI_j} \quad T_i/ISI_j > 0.4 \quad (17)$$

To scale the gain in proportion to initial linear segment, the gains estimated from Eq. 17 were divided by the value predicted for a normalized firing rate of 0.4.

A plot of the force sigmoid with the adjoining initial linear segment is shown in Fig. 2A. The peak gain occurred near the normalized rate of 1.0, and the value of the peak gain was approximately three times that of the low rate gain. The predicted force for a normalized input rate of 1.0 (Fig. 2A) was $\sim 85\%$ of maximum force, a value similar to that observed experimentally (Kernell et al. 1983b). In summary, the force gain for discharge j in unit i , calculated from Eq. 17, depended on the time interval from the preceding discharge and the twitch contraction time. This gain factor was then used to amplify the motor-unit impulse response (Eq. 12) for each discharge as

$$f_{ij}(t) = g_{ij} \cdot \frac{P_i \cdot t}{T_i} \cdot e^{1-(t/T_i)}. \quad (18)$$

FORCE RESPONSE TO A TRAIN OF DISCHARGES AND TOTAL MUSCLE FORCE. In any motor unit i and for a train containing k discharges, the force produced in the unit, $F_i(t)$, was equivalent to the sum of the individual impulse responses

$$F_i(t) = \sum_{j=1}^k f_{ij}(t - t_{ij}) \quad t - t_{ij} \geq 0 \quad (19)$$

The value of $f_{ij}(t - t_{ij})$ represents the force response to discharge j and was predicted from Eq. 18. Nonlinearities in the force response of motor units due to activation history, e.g., posttetanic potentiation (Burke 1981); the marked enhancement of twitch responses occurring with short-duration ISIs (doublet firing) (Burke et al. 1970); the serial dependence of twitch responses (Stein and Parmiggiani 1981) or fatigue (Bigland-Ritchie and Woods 1984) was not included in the model.

Modeled twitches and force responses to trains of stimuli (5, 10, 20, and 30 imp/s) for a small, slow unit ($P_i = 1.0$ force unit; $T_i = 90$ ms) are shown in Fig. 2B and are presented for a large, fast-twitch unit ($P_i = 100.0$ force units; $T_i = 30$ ms; stimulus trains: 10, 20, 30, 50, and 100 imp/s) in Fig. 2C. At a stimulus rate of 20 imp/s, the force of the slow unit was maximal, and stimulus rates beyond this level achieved no increase in force. For the fast unit of Fig. 2C, a stimulus rate of ~ 50 imp/s was required to attain full force output. The ratio of twitch force to maximum tetanic force was 0.11 for all units.

The mechanical coupling that may occur between active motor

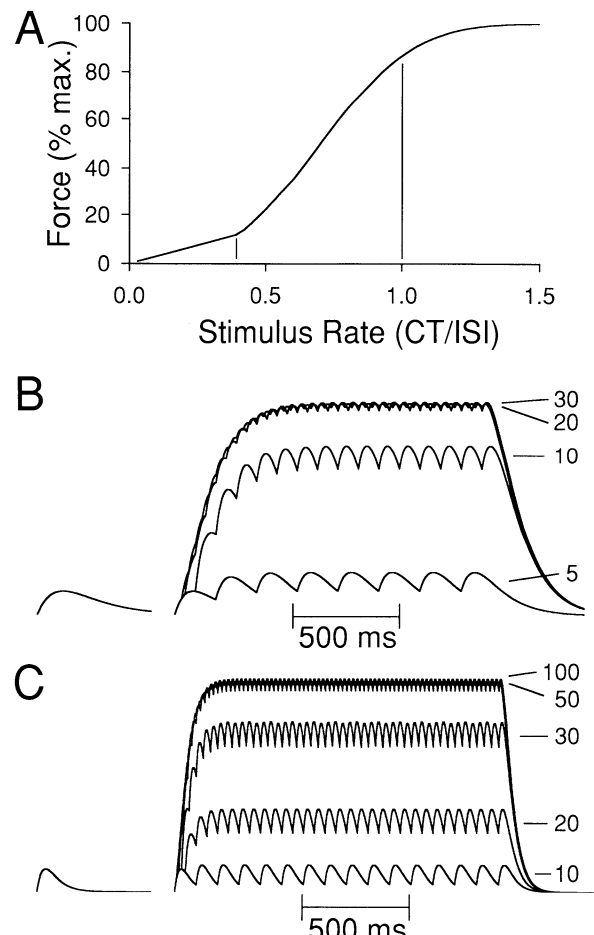


FIG. 2. *A*: simulated relation between stimulus rate and isometric force for motor units. The ISI (interstimulus interval) was normalized by dividing it by each unit's assigned contraction time, CT to become ISI/CT . The normalized stimulus rate was the inverse of the normalized ISI or CT/ISI . Motor-unit force increased linearly for normalized rates up through 0.4 (left vertical line). For stimulus rates beyond 0.4, force increased as a sigmoid function of rate, with the peak gain (ratio of force to stimulus rate) occurring at a normalized rate of 1.0 (right vertical line). *B*: simulated twitch (left trace) and superimposed responses to trains of stimuli (right traces) at 5, 10, 20, and 30 imp/s for a slow-twitch motor unit (contraction time = 90 ms). *C*: simulated twitch (left trace) and superimposed responses to trains of stimuli (right traces) at 10, 20, 30, 40, and 50 imp/s for a fast-twitch motor unit (contraction time = 30 ms). The force response of a motor unit was nonlinearly related to stimulus rate and depended on the contraction time of each unit.

units and that may lead to nonlinear force summation (Clamann and Schelhorn 1988) was not considered in the model. The mechanical actions of motor units were assumed to be independent of one another, thus the total force in the muscle, $F_M(t)$, was determined as the sum of the individual motor-unit forces

$$F_M(t) = \sum_{i=1}^n F_i(t) \quad (20)$$

Simulation of the surface EMG

The complex signal detected with surface electrodes during muscle contraction arises from the temporal summation of action potentials emanating from many active motor units. To simulate the surface-detected EMG, it was necessary to model those factors that affect the amplitude and shape of motor-unit action poten-

tials. Those included in the model, in addition to factors associated with electrode size, spacing, and configuration (Fuglevand et al. 1992), were the size and location of the motor-unit territories and the propagation velocity of the muscle-fiber action potentials.

MOTOR-UNIT TERRITORY. Differences in the force exerted by motor units could be due to variation in the cross-sectional areas of muscle fibers, the intrinsic force-generating capacity of the fibers, or the number of fibers innervated (Kanda and Hashizume 1992). In human muscle, there does not appear to be systematic differences in fiber diameter associated with fiber type (Lexell et al. 1988; Saltin and Gollnick 1983). Although differences have been reported in the force/cross-sectional area of different fiber (Mounier et al. 1989) and motor-unit types (Burke and Tsairis 1973; McDonagh et al. 1980), the main factor underlying the variation in motor-unit force appears related to fiber number (Bodine et al. 1987; Chamberlain and Lewis 1989; Kanda and Hashizume 1992; Tötösy de Zepetnek et al. 1992). In the model, therefore, all muscle fibers were assigned to have the same cross-sectional area, and the number of fibers innervated by each motor unit was directly proportional to the twitch force of the unit.

The fibers of a motor unit are scattered throughout a broad region of the muscle cross section (up to several millimeters in diameter) (Bodine et al. 1987; Buchthal et al. 1957; Burke 1981) and interdigitate with fibers belonging to many other motor units. The distribution of unit fibers within a motor units territory is relatively uniform (Stålberg and Antoni 1980) with densities reported to be 2–9 unit fibers/100 fibers (Burke 1981; Kanda and Hashizume 1992) or 20 unit fibers/mm² of muscle area (Armstrong et al. 1988). Regionalization of muscle-fiber types is seen in small mammals where slow twitch fibers tend to predominate near the muscle interior (Yellin 1969). The degree of regionalization in human muscle, however, is small (Johnson et al. 1973; Lexell et al. 1986; Milner-Brown and Stein 1975), and therefore it was assumed that a motor-unit territory could be located anywhere within the muscle cross section. The distribution of unit fibers within a territory was assumed to be uniform, and the density of unit fibers was assumed to be the same for all motor units. The motor-unit territories were modeled to be circular in shape.

The total number of fibers (n_f_{total}) in a muscle with cross-sectional area A_m , was estimated as $n_f_{\text{total}} = A_m/A_f$ where A_f was the average area of a muscle fiber. A theoretical total twitch force, P_{total} , was determined from the sum of the individual unit twitch forces, P_i (assigned in Eq. 13) as $P_{\text{total}} = \sum_{i=1}^n P_i$. The ratio $n_f_{\text{total}}/P_{\text{total}}$ represented the number of muscle fibers required to exert one unit of force (1 unit force \approx twitch force of smallest motor unit). The number of fibers innervated by each motor unit was then calculated as

$$n_f_i = (n_f_{\text{total}}/P_{\text{total}}) \cdot P_i \quad (21)$$

The area encompassed by each motor-unit territory, A_i , was then calculated from the unit fiber density, ϑ (unit fibers/mm² area of muscle), with the use of:

$$A_i = n_f_i / \vartheta \quad (22)$$

To establish the locations of the individual motor-unit territories, a Cartesian coordinate system was located at the center of a circular muscle cross section. The center of each motor-unit territory was generated as a random x , y coordinate pair but constrained such that no portion of the motor-unit territory exceeded the muscle boundaries. The coordinates were then transposed to an electrode axis system (for details, see Fuglevand et al. 1992). The electrode was assumed to lie on the skin surface, separated from the muscle by a subcutaneous layer of known thickness.

CONDUCTION VELOCITY. The speed at which action potentials are propagated along muscle fibers will inversely affect the duration of the detected motor-unit action potentials. Conduction velocities in human muscle fibers vary over a two- to fourfold range (2.6–5.3 m/s, Andreassen and Arendt-Nielsen 1987; 3.3–5.2 m/s, Buchthal et al. 1955; 2–6 m/s, De Luca 1979; 1.5–5.8 m/s, Stålberg 1966). Action-potential conduction velocity and contractile speed of a motor unit appear to be tightly coupled (Andreassen and Arendt-Nielsen 1987). Conduction velocities of simulated motor units therefore were computed from a simple linear (negative slope) relationship with the assigned motor-unit contraction times. The range of conduction velocities used was from 2.5 to 5.5 m/s.

MOTOR-UNIT ACTION-POTENTIAL SIMULATION. The manner by which individual muscle-fiber action potentials were simulated has been described in detail elsewhere (Fuglevand 1989; Fuglevand et al. 1992). Briefly, a dipole representation of the transmembrane current was used to simulate individual fiber action potentials in a three-dimensional muscle volume. The effects of anisotropic muscle conductance, innervation zone location, fiber length, electrode area, and electrode configuration were included in the fiber action-potential model. A motor-unit action potential was considered equivalent to the sum of its constituent muscle-fiber action potentials. A computational method, based on the concept of isopotential layers (Fuglevand et al. 1992), was used to estimate that sum.

An isopotential layer was defined as a thin element of muscle area such that any fiber lying within the element would, when active, cause a similar potential to be detected by the electrode. The trajectory of the isopotential path depended on the electrode geometry. The muscle cross section was divided into many isopotential layers, and one muscle-fiber action potential was simulated for each layer. Each motor-unit territory was traversed by a number of layers, and the area of each isopotential element within the boundaries of the motor-unit territory was calculated. The number of unit fibers within a isopotential element was computed from the product of the unit fiber density value (ϑ) and the element area. The muscle-fiber action potential corresponding to a particular layer was then scaled in amplitude by the number of unit fibers within the element to yield an element potential. The assigned conduction velocity of the motor unit was then used to temporally scale the element potential. This process was repeated for all isopotential elements contained within a motor-unit territory, and the motor-unit action potential was estimated as the sum of the element potentials.

Action potentials were simulated for 120 motor units innervating a total of 71,747 muscle fibers in a muscle having a cross-sectional diameter of 1.5 cm. Muscle-fiber diameter was 46 μm , and the motor-unit fiber density was 20 unit fibers/mm² area of muscle. The smallest motor unit innervated 28 fibers, the largest unit innervated 2,728 fibers, and the average innervation ratio was 598 fibers/motor unit. Bipolar surface electrodes (area = 4 mm², interelectrode distance = 11 mm), separated from the muscle by a subcutaneous layer of 1.5 mm, were used in the simulations. Simulated action-potential amplitude increased roughly in proportion ($r^2 = 0.655$) with motor-unit twitch force (Fig. 3), similar to experimental findings (Goldberg and Derfler 1977). The variability in the relationship shown in Fig. 3 was due to the random locations of the motor-unit territories within the simulated muscle cross section.

A train of motor-unit action potentials was created by including an action-potential waveform for each discharge of the unit predicted by the motoneuron pool model. The EMG signal was then generated by summing, at each instant in time, all the motor-unit action-potential trains. The resulting EMG signal was high-pass

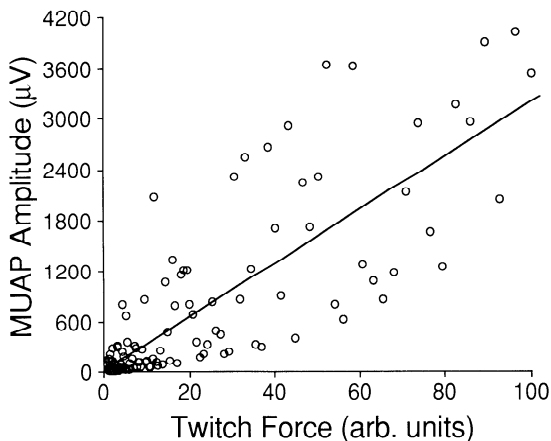


FIG. 3. Plot of the peak-to-peak amplitude of motor-unit action potentials as a function of twitch force for the population of 120 simulated motor units. Action-potential amplitude increased linearly with motor-unit twitch force (linear regression line shown, $r^2 = 0.655$). The variability in the relation was due to the random locations of motor-unit territories within the muscle cross section.

filtered with the use of a first-order digital filter with a cutoff frequency of 5 Hz to simulate the A-C coupling of bioamplifiers.

Example outputs of the three model components are shown in Fig. 4. The top of Fig. 4 shows the discharge times of every 10th motoneuron in the pool of 120 for an excitatory drive function that increased linearly in the 1st s to a level just sufficient to recruit the 120th neuron. Excitation was then maintained constant for the remainder of the simulation period. The surface EMG and muscle force signals simulated from the neural input represented in the top of Fig. 4 are shown in the middle and bottom of the figure, respectively.

Simulation procedures

Two recruitment and three firing-rate conditions were tested in the simulations. The recruitment conditions were 1) low recruitment range (upper limit of recruitment <50% maximum excitation) and 2) broad recruitment range (upper limit of recruitment >70% maximum excitation). The firing rate conditions involved variation in the peak firing rates (PFR) of the motoneurons. In one set of simulations, early recruited motoneurons were assigned higher PFRs than later recruited ones (see Eq. 5). In another set of simulations, all motoneurons were assigned the same value of PFR. And in the third set the PFR of each neuron was matched to the mechanical properties of its muscle unit. In this case the PFR for each unit was set at the stimulus frequency required to just attain maximum tetanic force, i.e., at a normalized stimulus rate of 1.5 (see Fig. 2). Therefore, for *motor unit 1*, which had a contraction time of 90 ms (Fig. 1B), the PFR was 16.7 imp/s, and the PFR for *motor unit 120*, which had a contraction time of 30 ms (Fig. 1B), was 50 imp/s.

For each combination of recruitment and firing rate conditions, muscle force and surface EMG signals were simulated at 11 levels of steady-state excitation: at 5% maximum excitation and from 10 to 100% maximum excitation in 10% increments. Maximum excitation was defined for each set of simulations as the level of excitatory drive required to bring the last recruited neuron to its assigned peak firing rate. The duration of each simulation period (i.e., for each level of excitation) was 10 s. The EMG was simulated at an effective rate of 5,000 samples/s and force at 500 samples/s. The muscle was composed of 120 motor units with twitch parameters assigned according to the schedule shown in Fig. 1B and with action-potential amplitudes as indicated in Fig. 3.

At each level of excitatory drive and for each condition, the

average force and the average rectified EMG were determined over the 10-s simulation period. The initial 1 s of force was not included in the averages because of the lag in force development to a steady state under constant excitation. The values of the average EMG and average force were expressed as percentages of the values obtained under maximum excitation defined for each condition. The relationships between EMG and excitation and between force and excitation were determined, and then EMG values were plotted against the corresponding force for each level of excitation. The EMG-force data points were then fit as a linear or curvilinear relationship depending on the following criteria. First, linear regression was used to find the line of best fit through the data. If the linear model accounted for >99% of the variance in the data ($r^2 > 0.99$), then a linear relationship was assumed to be an adequate representation of the data. Otherwise, polynomial regression (2nd order or larger) was used to fit the data ($r^2 > 0.99$). If the polynomial, however, did not provide a significant ($P < 0.05$) improvement in the fit of the data over the linear model, then the linear representation was used. Last, the force at which the last unit was recruited was estimated with the use of linear interpolation. The upper limit of recruitment therefore was identified both in terms of maximum force and in terms of maximum excitation.

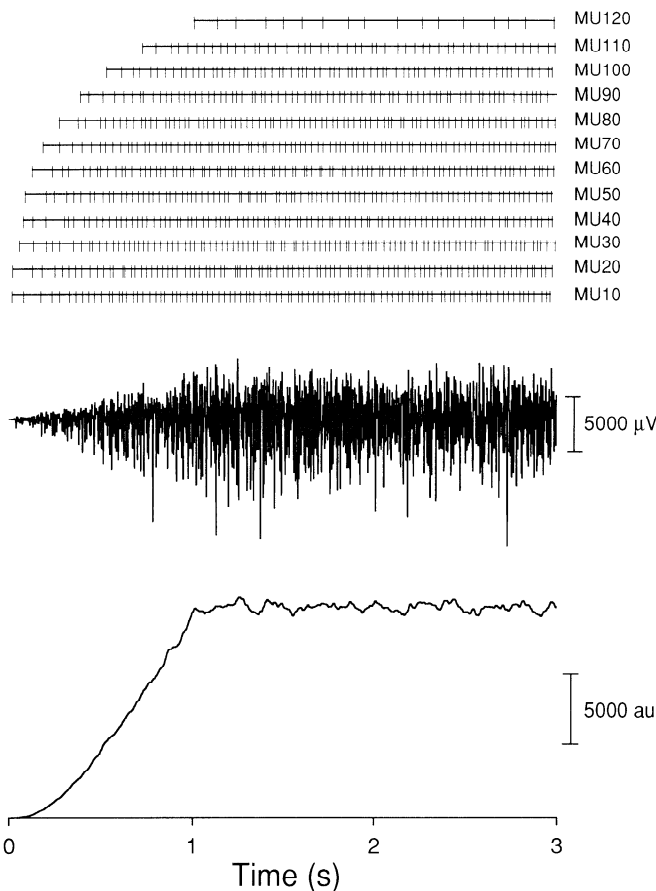


FIG. 4. Example output of the motor-unit model. The top set of traces show the firing times (indicated by vertical strokes) of every 10th motor unit in the pool of 120 units in response to excitatory drive that increased linearly over the initial 1 s of the simulation period to a level just sufficient to recruit the 120th motor unit. The excitatory drive was then maintained constant for the remainder of the simulation. The middle trace shows the simulated electromyogram (EMG) as detected by bipolar surface electrodes (4 mm² area, electrode separation = 11 mm), and the bottom trace shows the simulated muscle force that resulted from the neural input depicted in the top set of traces. Calibration for force in arbitrary force units (au).

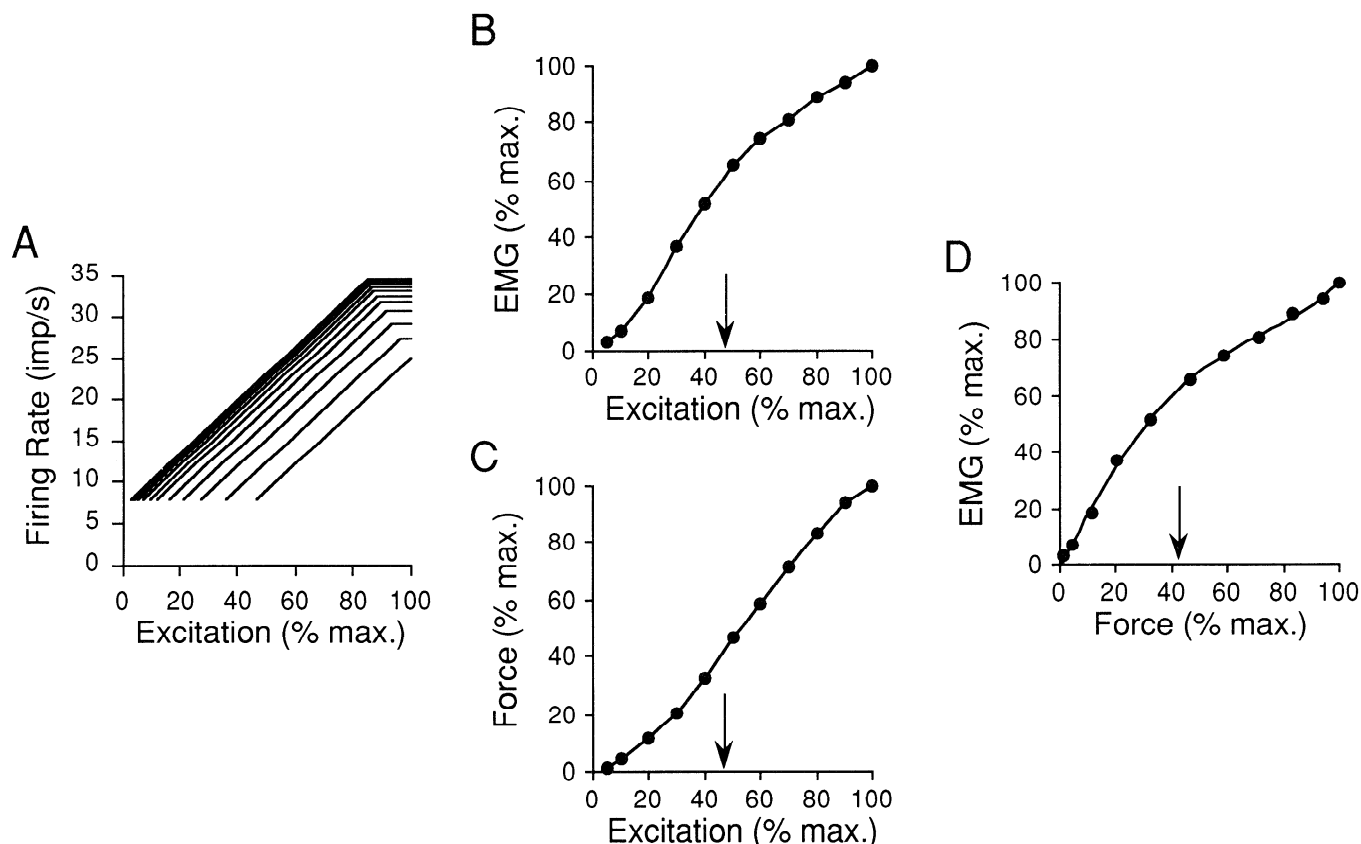


FIG. 5. Simulation results from narrow recruitment-range condition with peak firing rates inversely related to recruitment threshold. *A*: schematic diagram showing relation between excitatory drive and firing rate for every 10th motoneuron from the 10th (leftmost path) to the 120th (rightmost path). Peak firing rates ranged from 35 imp/s (*unit 1*) to 25 imp/s (*unit 120*). *B*: relationship between surface EMG and excitatory drive. *D*: relationship between force and excitatory drive. Each point plotted represents the average-rectified EMG (*B*) or average force (*C*) calculated from a 10-s simulation period at each level of steady-state excitation. EMG and force were expressed as percentages of values obtained during the maximum excitation condition. The last unit was recruited at 46.9% of maximum excitation (arrows). *D*: plot of EMG as a function of force for each level of excitatory drive. Force at which the last unit was recruited (arrow) was calculated by linear interpolation to be 42.0% of maximum force. This form of EMG-force relationship is not generally seen experimentally.

RESULTS

PFRs inversely related to recruitment threshold

NARROW RECRUITMENT RANGE. The organization of neural input for the condition where early recruited units attained higher firing rates than later recruited units and where recruitment operated over a narrow range is depicted in a schematic diagram in Fig. 5*A*. Each trace depicts the change in firing rate with excitation for individual neurons (for clarity, only every 10th neuron is shown). For example, the 110th neuron (*2nd trace from the right*) remained inactive until excitation reached $\sim 36\%$ of maximum at which time the neuron discharged at a rate of 8 imp/s. When excitation increased above this recruitment threshold level, the neuron increased its firing rate in a linear way with a slope similar to all other neurons. PFR was attained for the 110th neuron at an excitation of $\sim 96\%$ of maximum at which point it no longer responded to further increases in excitation. The range of PFRs used in this simulation (*unit 1* to *unit 120*) was 35–25 imp/s. Recruitment was complete at 46.9% of maximum excitation, and the mean firing rate at maximum excitation was 31.6 imp/s.

Within the recruitment range, an increase in excitation

effected two alterations in the neural input to muscle. It caused an increase in the firing rate of active units and recruited additional units with larger action-potential amplitudes and force capacities. For this reason, the EMG increased steeply with excitation within the recruitment range (Fig. 5*B*, arrow on abscissa indicates excitation at which last unit was recruited). Beyond the upper limit of recruitment, increases in excitation caused alteration only in firing rates. For this reason, EMG increased at a somewhat lower rate in the range of excitations above the recruitment limit.

Force also increased progressively within the range of excitations where recruitment operated (Fig. 5*C*) but at a rate somewhat lower than the EMG. In this region, units that had the capacity for generating large forces were firing at low rates. These large force units also had the briefest twitch contraction times (Fig. 1*B*). Hence these units were operating in the low force portion of their force-frequency curves (Fig. 2). The relatively larger value of EMG compared with force over the recruitment range caused the EMG-force relation for this condition (Fig. 5*D*) to have an initial steep slope. The steepest portion of the force-excitation curve (Fig. 5*C*) occurred between 40 and 80% of maximum excitation. The increased firing rate in this range brought many units into the high-gain portion of their force-frequency

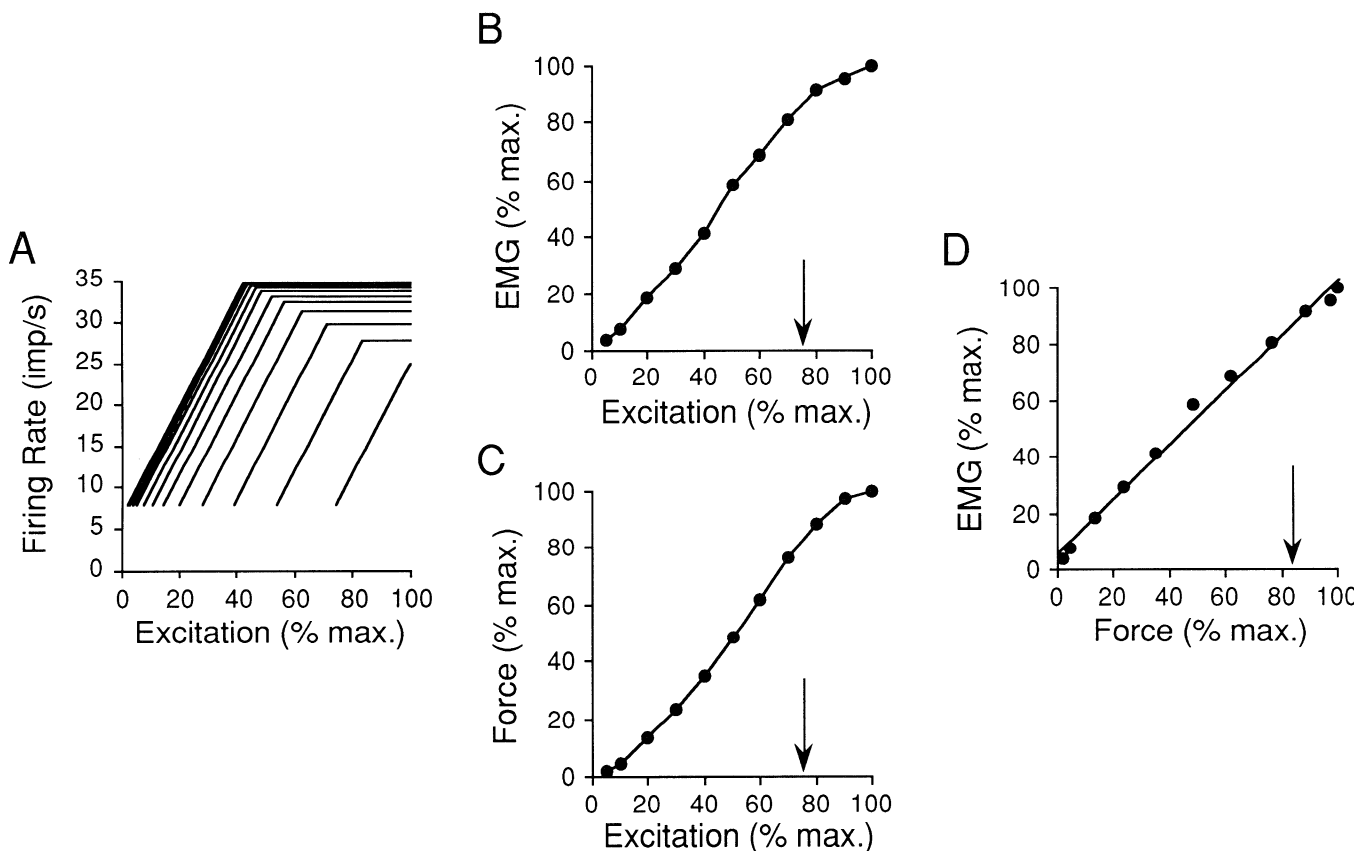


FIG. 6. Simulation results from broad recruitment-range condition with peak firing rates inversely related to recruitment threshold. See Fig. 5 for detailed legend. The last unit was recruited at 74.6% of maximum excitation (arrows in *B* and *C*) or 81.9% of maximum force (arrow in *D*). The similarity in the forms of the EMG-excitation (*B*) and force-excitation (*C*) curves caused the EMG-force relation (*D*) to be linear ($r^2 > 0.99$) and consistent with that observed in some human muscles.

curves. EMG plotted as a function of force for these excitation levels therefore had a lower slope than the initial portion of the EMG-force relationship (Fig. 5*D*). An attenuation in the slope of the force-excitation curve was seen for excitation $>80\%$ of maximum (Fig. 5*C*). The reduction in force slope in the upper excitatory range was primarily due to an increasing number of units operating within the plateau portion of their force-frequency curves. Because the slope of the EMG-excitation curve was relatively uniform at high excitation levels (e.g., Fig. 5*B*) and the force-excitation slope attenuated slightly, the plot of EMG as a function of force (Fig. 5*D*) displayed a tendency for a terminal increase in slope.

BROAD RECRUITMENT RANGE. The schematic diagram representing the pattern of neural input for a broad recruitment range with PFRs inversely related to recruitment threshold is presented in Fig. 6*A*. For this set of simulations, recruitment operated over 75% of the excitatory range. Increased excitation up to $\sim 40\%$ of maximum caused increases in both recruitment and firing rate. The slope of EMG-excitation relation (Fig. 6*B*) progressively increased throughout most of this range, in a way similar to that described for the narrow recruitment range condition in Fig. 5. For excitation levels from 40 to 80% of maximum, the tendency for a continued increase in the slope of the EMG-excitation relationship was offset by an increase in the number of units that reached their peak firing rate.

Thus EMG-excitation slope stabilized in the intermediate range of excitation. Beyond the upper limit of recruitment, increased excitation had only one effect, increasing firing rates in the subpopulation of large units that had not yet attained peak firing rates. Thus increased excitation in the range above 80% of maximum only moderately increased EMG amplitude.

The shape of the force-excitation curve (Fig. 6*C*) associated with a broad recruitment range was qualitatively similar to that associated with the condition of narrow recruitment range (Fig. 5*C*). The two main differences were that, in the broad recruitment range condition (Fig. 6*C*), force increased slightly more rapidly in the initial excitation range, and the plateau in force at high excitation was more prominent. Firing rates increased more rapidly for a given change in excitation in this condition (Fig. 6*A*). Therefore, in the low excitation range, active motor units, although fewer in number, were driven more quickly up their force-frequency curves causing the total force to rise initially to slightly higher levels compared with the narrow recruitment range condition. For example, at 20% maximum excitation, force was 13.0% of maximum for the broad recruitment condition (Fig. 6*C*) and 11.1% for the narrow recruitment condition (Fig. 5*C*). Also, because the increase in firing rate was relatively steeper for the broad recruitment condition, units achieved their peak firing rates at lower excitation levels. At $\sim 80\%$ of maximum excitation, most of the units had reached peak firing rate in the broad

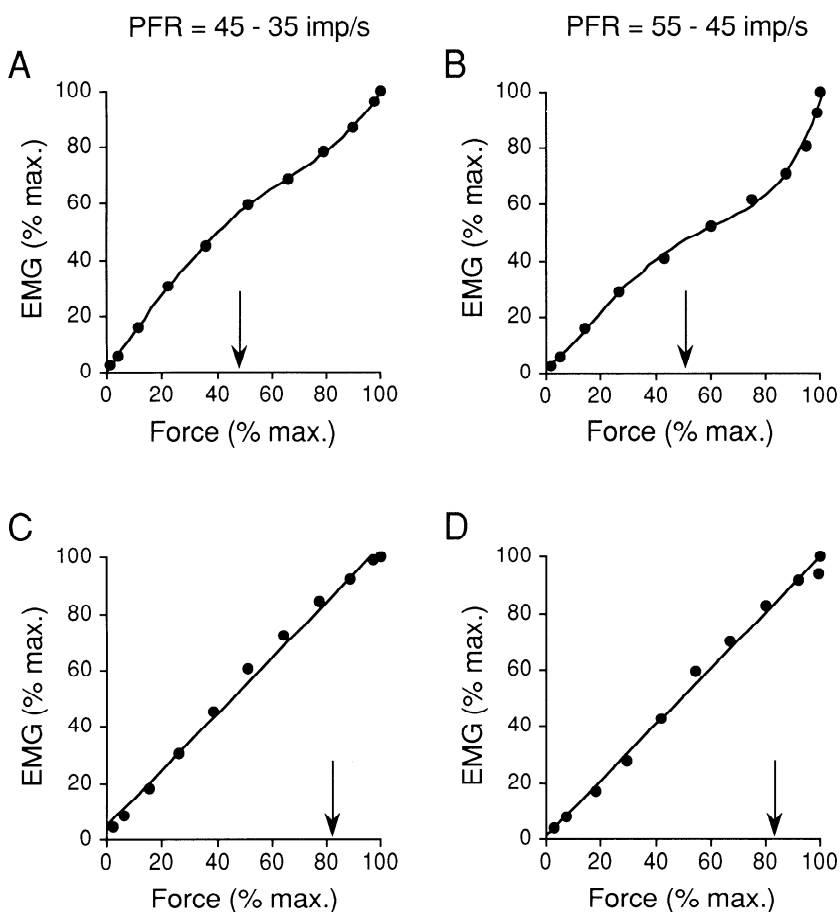


FIG. 7. EMG-force relationships for narrow (*A* and *B*) and broad (*C* and *D*) recruitment range conditions. Peak firing rates (PFR) were inversely related to motor-unit recruitment threshold and ranged (unit 1 to unit 120) from 45 to 35 imp/s (*A* and *C*), and from 55 to 45 imp/s (*B* and *C*). Arrows on force axes show predicted force at which last unit was recruited for each condition (*A*, 47.9%; *B*, 51.2%; *C*, 81.1%; *D*, 83.6% of maximum force). When recruitment operated over a narrow range (*A* and *B*, also Fig. 5*D*), the EMG-force relation was nonlinear and dissimilar to that observed experimentally. When recruitment operated over a broad range (*C* and *D*, also Fig. 6*D*), the relationship between EMG and force was linear.

recruitment condition, whereas none were at peak firing rate in the narrow recruitment condition. Therefore the terminal plateau in force development was more pronounced in the broad recruitment condition as compared with the narrow recruitment condition. When EMG was plotted as a function of force (Fig. 6*D*), the relationship had a linear form because of the similarity in the shapes of the EMG-excitation (Fig. 6*B*) and force-excitation curves (Fig. 6*C*).

SENSITIVITY OF EMG-FORCE RELATIONSHIPS TO PEAK FIRING RATE LEVEL. The EMG-force relationships shown in Fig. 7, *A* and *B*, were derived from simulations where recruitment was confined to a narrow range and peak firing rates ranged (unit 1 to unit 120) from 45 to 35 imp/s (Fig. 7*A*) and from 55 to 45 imp/s (Fig. 7*B*). The organization of neural input for Figs. 7, *A* and *B*, was like that depicted in Fig. 5; the difference being in the magnitude of the PFR. Likewise, the EMG-force relationships presented in Fig. 7, *C* and *D*, where recruitment operated over a broad range and with PFR of 45–35 imp/s (Fig. 7*C*) and 55–45 imp/s (Fig. 7*D*), had a neural input scheme like that shown in Fig. 6. For the narrow recruitment range conditions (Figs. 5*D* and 7, *A* and *B*), the EMG-force relationships were curvilinear and of a form not typically observed experimentally. In contrast, when recruitment operated over a broad range (Figs. 6*D* and 7, *C* and *D*), linear EMG-force relationships like that seen experimentally in a number of muscles were exhibited. The general form of the EMG-force relationships therefore appeared not to depend on the particular PFR range selected.

Equivalent PFRs

The results of the simulations in which all motor units were assigned the same PFR (41.6 imp/s) are shown in Fig. 8. A PFR of 41.6 imp/s was selected because it was equivalent to the mean firing rate at maximum excitation for the intermediate PFR conditions shown in Figs. 7, *A* and *C*. For the narrow recruitment range condition, the schematic diagram representing the organization of neural input is shown in Fig. 8*A*, and the EMG-force relationship is presented in Fig. 8*B*. Similarly, the neural input scheme and the EMG-force relationship are shown for the broad recruitment range condition in Figs. 8, *C* and *D*, respectively. The simulation with a narrow recruitment range had an EMG-force relationship (Fig. 8*B*) similar to that of other simulations with narrow recruitment ranges (Figs. 5 and 7, *A* and *B*) but with a more prominent increase in EMG at high force levels.

When a broad recruitment range was implemented, the EMG-force relationship (Fig. 8*D*) had a form approaching the nonlinear shape observed in some muscles. The parameters of neural input were not substantially different from those that yielded the linear EMG-force relationships (Fig. 6). A surprising result of these simulations was that the absolute value of the EMG was substantially augmented under the condition where the mean firing rates of the motor units attained a similar value. The average rectified value of the EMG under maximum excitation for the simulation shown in Fig. 8*D* was 4,201.6 μ V. For the simulations represented in Fig. 7*C*, in which the population mean

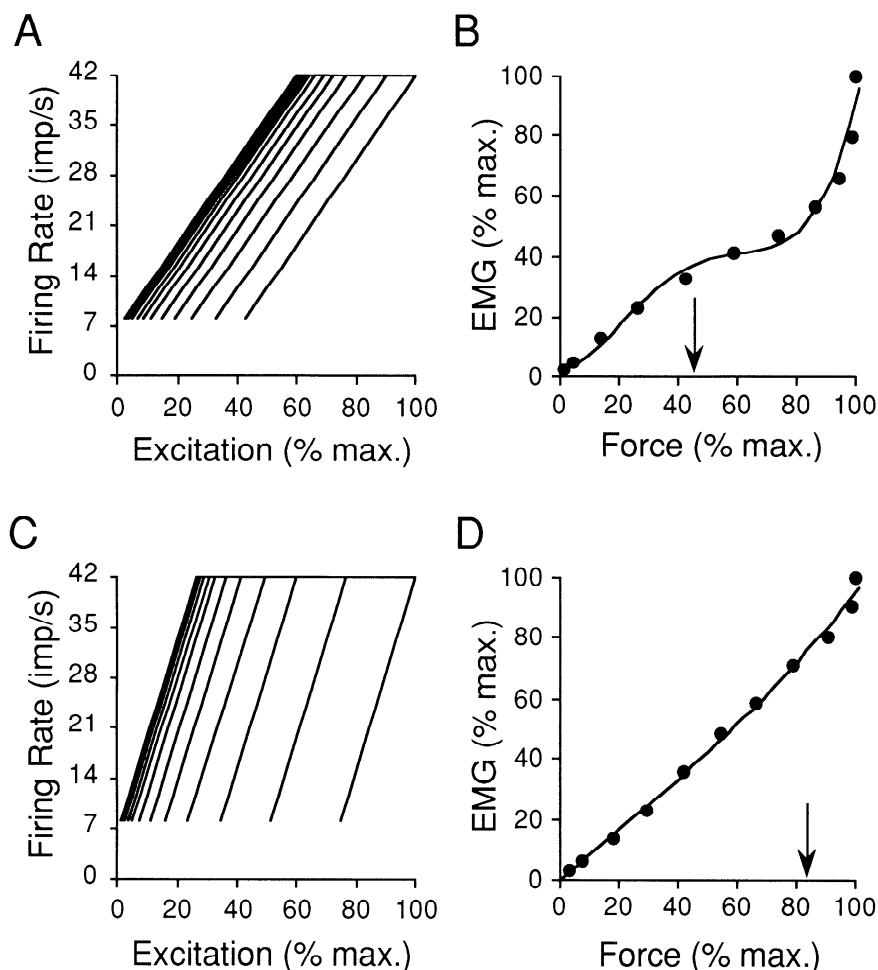


FIG. 8. Simulation results for condition where all motor units were assigned the same peak firing rate (41.6 imp/s) and recruitment operated over narrow (*A* and *B*) or broad (*C* and *D*) ranges. *A* and *C*: schematic diagrams showing relation between excitatory drive and firing rate for every 10th motoneuron from the 10th (leftmost path) to the 120th (rightmost path). *B* and *D*: EMG-force relationships for narrow and broad recruitment conditions, respectively. Estimated force at which last unit was recruited is indicated by arrow on force axis (*B*, 46.0%; *D*, 84.2% of maximum force). The EMG-force relationship was nonlinear and unlike that seen experimentally when recruitment operated over a narrow range (*B*). When recruitment operated over a broad range (*D*), the EMG-force relationship tended toward a parabolic form observed in some muscles.

firing rate at maximum excitation was the same as that used for Fig. 8*D* but where the peak rates were dispersed over the range 45–35 imp/s, the value of maximum EMG was 2,640.4 μ V, 63% of the value attained in Fig. 8*D*. One might expect the value of maximum EMG in Fig. 7*C* to be somewhat less, because in that set of simulations, the units with the largest action potentials discharged at the lowest rates, namely, near 35 imp/s. However, the value of maximum EMG from the simulations of Fig. 8 was also larger than that obtained from other simulations where all the motor units discharged at higher rates. The firing rates at maximum excitation for the condition shown in Fig. 7*D* ranged from 55 to 45 imp/s (mean rate = 51.6 imp/s). The value of the rectified average EMG for this condition, however, was only 3,391.0 μ V, 81% of the value obtained in Fig. 8*D*, where all units discharged at 41.6 imp/s.

This augmentation in the EMG signal appeared to be related to the bursting behavior that was evident in the simulated EMG as mean firing rates approached a similar value. Figure 9*A* shows a 500-ms segment of simulated EMG from the maximum excitation condition of Fig. 7*C* in which the mean firing rates were dispersed over the range 45–35 imp/s. The EMG segment in Fig. 9*B*, which shows large fluctuations in amplitude occurring at regular intervals, is from the maximum excitation condition of Fig. 8*D*, where all units discharged at a mean rate of 41.6 imp/s. For the simulations in Fig. 8, the firing rates of the units progressively converged toward the same value as excitation in-

creased. Therefore the degree of EMG signal augmentation associated with bursting increased as excitation increased. In the simulations depicted in Fig. 8*D*, this progressive enhancement in EMG amplitude induced a slight parabolism on what otherwise would have been a linear EMG-force relationship.

PFRs matched to mechanical properties

The patterns of neural input used in simulations where PFRs were determined for each unit from the stimulus rate required for maximum tetanic force (see Fig. 2) are shown in Figs. 10, *A* and *C*, for narrow and broad recruitment ranges, respectively. Although the EMG-force data from the two recruitment schemes were not widely different, a polynomial fit provided a significant improvement ($F = 13.42$, $P < 0.01$) over a linear model in accounting for variance in the data for Fig. 10*B* but not for the data in Fig. 10*D* ($F = 4.13$, $P > 0.05$). Thus, despite the contrast of these firing rate schemes (Figs. 10, *A* and *C*) with those of Figs. 5*A* and 6*A*, the EMG-force relationships followed similar patterns. A nonlinear form resulted when the recruitment range was narrow (Fig. 10*B*) and a linear EMG-force relationship emerged from the broad recruitment range condition (Fig. 10*D*).

An unexpected result of these simulations was that the maximum force for these conditions was less than the maximum force capacity of the system. The maximum force

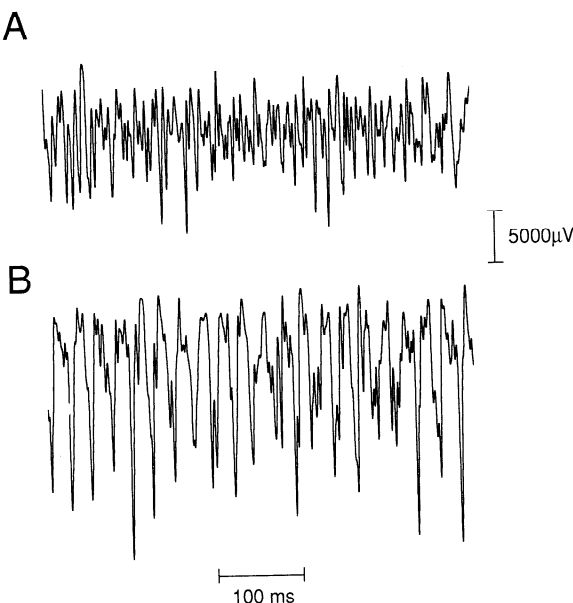


FIG. 9. Simulated surface EMG during maximum excitation for conditions where peak firing rates were dispersed over a range of values (*A*) or where all units were assigned the same mean peak firing rate (*B*). Duration of each EMG segment was 500 ms. Firing rates used in *A* varied over the range 45–35 imp/s (mean 41.6 imp/s). In *B*, all units discharged with a mean rate of 41.6 imp/s. Large fluctuations in EMG at regular intervals of 24 ms (equivalent to period for 41.6 Hz) are evident in *B*. These bursts in EMG occurred despite that the sequence of discharge times was independently and randomly determined for each unit and that the variability in interspike intervals was broad (coefficient of variation, 20%). The amplitude of the EMG was substantially larger in the condition where all units discharged with the same mean rate [rectified average EMG 2,640.4 μ V for dispersed (*A*) and 4,201.6 μ V for same peak firing rate (*B*) conditions].

capacity was calculated simply as the sum of the maximum forces under tetanic stimulation for all units in the pool. For the population of 120 motor units used in this investigation, this calculation yielded a value of 23,878 force units. The maximum force for the matched firing rate conditions shown in Fig. 10*D* was 20,616 force units or 86% of the maximum force capacity. This result may seem paradoxical given that each unit was assigned a PFR equivalent to the stimulus rate required for maximum tetanic force. However, it appears that variability in the ISIs combined with a nonlinear force-frequency relationship caused the force at maximum excitation to be less than the maximum capacity.

This effect is depicted in Fig. 11. Each unit was modeled to have its own force-frequency curve that depended on its contraction time. At a particular constant-interval stimulus rate (SR_m , bottom of Fig. 11), maximum force for that unit was achieved. This rate was calculated for each unit as 1.5 divided by the contraction time (s) of the unit (see Fig. 2). To emulate the discharge patterns seen during voluntary activity, the actual discharge times used to drive the force model were simulated as a random process having a Gaussian distribution with a mean ISI equivalent to the inverse of the predicted firing rate. Therefore, in the case of a unit discharging at its peak rate, the mean ISI (ISI_m , top of Fig. 11) was equivalent to $1/SR_m$. Approximately one-half of the ISIs would be less than ISI_m and therefore would be associated with firing rates greater than SR_m . These short

ISIs were ineffective to enhance force because the associated frequencies resided in the plateau region of the force-frequency curve. On the other hand, ISIs longer than ISI_m tended to decrease force because the firing rates associated with these long intervals fell somewhere on the shoulder of the force-frequency curve. Thus the average force over the trial was something less than maximum force capacity of the unit. The mean rate of voluntary discharge required to achieve maximum force would therefore need to be higher than that expected from constant interval stimulation to keep most ISIs in the plateau region of the force-frequency curve.

Recruitment threshold, twitch force, and force contribution due to recruitment

Individual motor-unit twitch forces plotted as a function of the muscle force at which each unit was recruited (threshold force) has often been presented in the experimental literature to help characterize the organization of motor-unit pools (e.g., Milner-Brown et al. 1973b; Stephens and Usherwood 1977; Thomas et al. 1987). Example correlates to those empirically derived plots are shown in Fig. 12*A*. These data were obtained from the simulations shown in Figs. 5 and 6, namely, for narrow and broad recruitment ranges with PFRs inversely related to recruitment thresholds. The results presented in Fig. 12 were not different when other PFR schemes were tested. Each point plotted in Fig. 12*A* shows the twitch force of the last-recruited unit as a function of the muscle force produced for different levels of excitatory drive. The data in Fig. 12 were obtained for only those excitatory drive conditions over which recruitment operated. The relationship between twitch force and the muscle force at which units were recruited was essentially linear for both recruitment conditions, similar to experimental findings.

The average force contributed by the most recently recruited unit to the overall muscle force declined hyperbolically as force levels increased (Fig. 12*B*). The linear relationship between twitch force and the threshold force of recruitment in Fig. 12*A* would seem to imply that the increment in force due to recruitment, relative to the existing muscle force, should be a constant across the force range (Harrison 1983; Milner-Brown et al. 1973b). However, the force contributed by a newly recruited motor unit depended not only on its twitch force but also on its response to the threshold firing rate. The threshold firing rate was set for all units at 8 imp/s. For low-threshold units with long contraction times, 8 imp/s was sufficient to produce >50% of maximum tetanic force (Fig. 2*B*). For high-threshold units with rapid contraction times, 8 imp/s caused <10% of maximum tetanic force to be exerted (Fig. 2*C*). Therefore the relative increment in force due to recruitment was not invariant but diminished substantially as recruitment progressed from low- to high-threshold units.

DISCUSSION

The relationship between EMG and force is linear in some human muscles and has a nonlinear form with a progressive increase in slope in others (Lawrence and De Luca 1983; Woods and Bigland-Ritchie 1983). It has been sug-

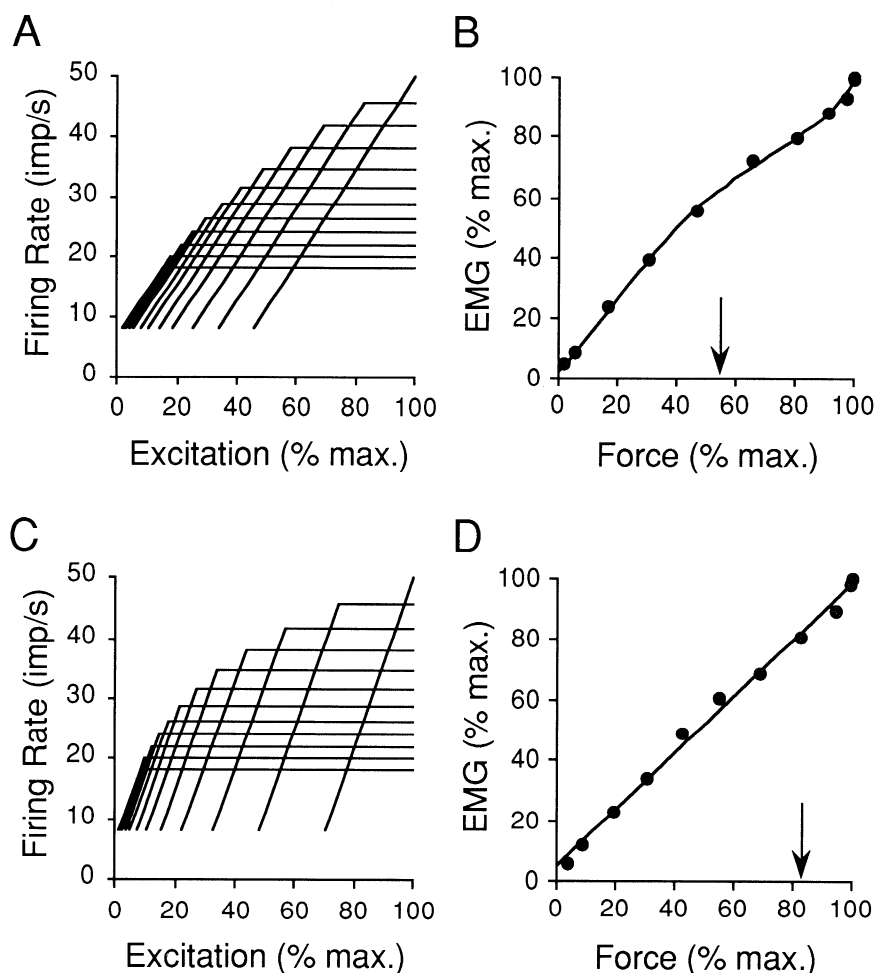


FIG. 10. Simulation results for the condition where the peak firing rate of each unit was set to the stimulus rate required for maximum tetanic force and recruitment operated over narrow (*A* and *B*) or broad (*C* and *D*) ranges. *A* and *C*: schematic diagrams showing relation between excitatory drive and firing rate for every 10th motoneuron from the 10th (leftmost path) to the 120th (rightmost path). *B* and *D*: EMG-force relationships for narrow and broad recruitment conditions, respectively. Estimated force at which last unit was recruited is indicated by arrow on force axis (*B*, 56.9%; *D*, 82.7% of maximum force). The EMG-force relationship was nonlinear and unlike that seen experimentally when recruitment operated over a narrow range (*B*). When recruitment operated over a broad range (*D*), the EMG-force relationship was linear, similar to other simulations using a broad recruitment range (Figs. 6*D* and 7, *C* and *D*).

gested that differences in the force range over which recruitment operates may be the main factor shaping the two types of EMG-force relationships (Lawrence and De Luca 1983; Solomonow et al. 1986). Linear relationships are thought to be exhibited in muscles where motor-unit recruitment is confined to a relatively narrow force range, whereas the nonlinear form is thought to emerge in muscles where recruitment operates over a broad force range. Both forms of the EMG-force relationship were simulated in the present study but only under the condition of a broad recruitment range. In all cases tested, narrow recruitment ranges (upper limit of recruitment <57% maximum force) produced EMG-force relationships that were unlike those observed experimentally. Therefore these results suggest that motor-unit pools may be organized such that recruitment operates over a large proportion of the force range for human skeletal muscle. Furthermore, the simulations indicated that the difference between muscles that exhibit the linear as opposed to the nonlinear form of the EMG-force relationship may be related to differences in firing rate behavior rather than due to differences in recruitment organization.

Rate coding organization

Three general approaches were taken for assigning PFRs. For the simulations depicted in Figs. 5–7, PFRs were based on the experimental findings indicating that low-threshold motor units attain higher firing rates than later recruited units (De Luca et al. 1982; Freund et al. 1975; Hoffer et al.

1987; Mellah et al. 1990; Monstera and Chan 1977; Tanji and Kato 1973). In a second set of simulations (Fig. 10), PFRs were matched for each unit to the stimulus rate necessary for maximum tetanic force. This type of firing rate organization, although intuitively appealing because it avoids the problem of overdriving motoneurons (Heckman and Binder 1991; Kernell 1992), has less empirical support (cf. Gyridov and Kosarov 1974). The degree of empirical support, however, for different firing rate organizations should not necessarily be taken to reflect likelihood of physiological existence. This is because it is nearly impossible, at present, to follow the discharge rate of a motor unit from recruitment onset up through maximum voluntary force. The simulated EMG-force relationships were linear for both types of firing rate assignments under the condition of a broad recruitment range. Therefore, on the basis of the criteria of comparing simulated EMG-force relationships to those observed experimentally, it was not possible to distinguish which of these two types of rate coding schedules was a more likely representation of the actual organization.

A third approach was to assign all units the same value of PFR (Fig. 8). In this case, and when a broad recruitment range was employed, EMG increased more rapidly at high force levels than at lower force levels, somewhat like that observed in human biceps brachii (Komi and Buskirk 1972; Lawrence and De Luca 1983; Vredenbregt and Rau 1973; Woods and Bigland-Ritchie 1983) and deltoid (Lawrence and De Luca 1983). Some experimental data

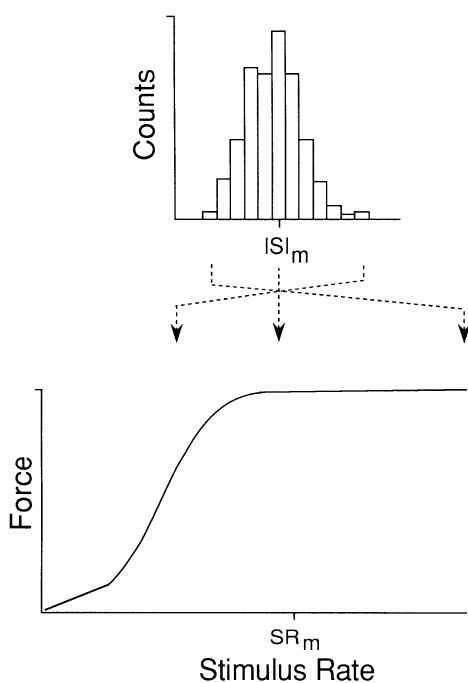


FIG. 11. Schematic diagram depicting how variability in interspike intervals may cause average force to be less than that produced with constant interval stimulation. Interspike interval histogram (*top*) for simulated voluntary activity in a motor unit discharging at a mean rate equivalent to the stimulus rate required to achieve maximum tetanic force (SR_m , *bottom*). Intervals shorter than the mean interval (ISI_m) cause the instantaneous firing rate to increase above SR_m (dashed line going from left to right). These high rates do little to enhance force because they reside in the plateau region of the force-stimulus rate curve. Firing rates associated with longer intervals (dashed line going from right to left), however, will tend to decrease force because these rates lie along a descending portion of the force-stimulus rate curve. The average force over a trial therefore will be less than what would be produced with constant interval stimulation.

from these two muscles also suggest that the PFRs of low- and high-threshold units are similar (De Luca et al. 1982; Kukulka and Clamann 1981).

When motor units discharged with similar mean rates, the simulated surface EMG signal (Fig. 9) demonstrated the phenomenon of cyclic bursting (Taylor 1962), which appeared to augment the value of the rectified average EMG. The bursting occurred even though the sequence of discharge times were randomly and independently determined for each unit. This phenomenon might be explained as follows. Two units that discharge independently will occasionally, due to chance, discharge at about the same time. If these units also discharge with the same mean rate and with similar Gaussian distributions of ISIs, then there is a high probability that the subsequent discharge in the two units will be near the same time. This effect becomes amplified as the number of units discharging with similar mean rates increases. The probabilistic increase in grouping of discharges induces some reinforcement in the summation of action potentials leading to an overall enhancement in the signal amplitude. Thus, as excitation increased and more units discharged near the same rate, the degree of EMG signal augmentation also increased.

It has been postulated that nonlinear EMG-force relationships might be due to an increasing degree of motor-unit synchronization as force levels increase (Komi and Buskirk 1972; Person and Libkind 1970). The essence of that suggestion was supported by the results of the present simulations. However, the EMG bursting seen in the pres-

ent simulations, and also likely to occur under some experimental conditions, was purely a chance phenomenon arising from independently discharging units with similar mean rates (Taylor 1962). This type of behavior, for which we have used the term bursting, should be distinguished from the term synchronization, which generally refers to the occurrence of near-coincident discharges in two or more neurons, *in excess of chance*, due to shared synaptic input from axonal branches of common presynaptic sources (Nordstrom et al. 1992). Nonetheless, the simulations illustrated that the amplitude of the surface EMG depends not only on the number of units active and their firing rates but also on the relative dispersion in mean firing rates across the population of active units.

Recruitment organization

The argument has been made that a narrow recruitment range might be beneficial to muscles, like the intrinsic muscles of the hand, that are utilized in precise gradation of

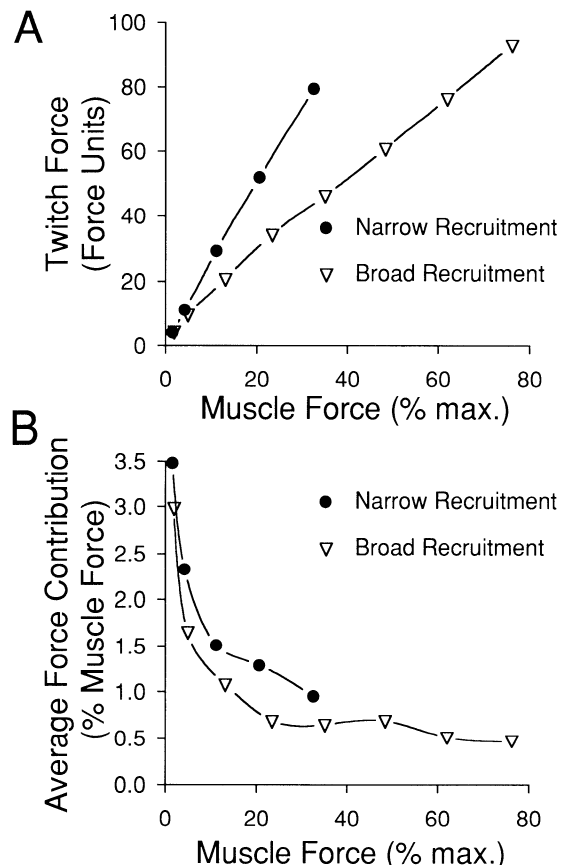


FIG. 12. *A*: twitch force of last-recruited motor units at different levels of muscle force for the narrow (●) and broad (▽) recruitment range conditions shown in Figs. 5 and 6, respectively. For the narrow recruitment range (●) the points plotted are from the excitatory drive conditions 5–40% maximum excitation, and the uppermost point represents the 114th unit in the pool of 120. The data for the broad recruitment condition (▽) were from the excitatory drive conditions 5–70% maximum excitation, and the last point plotted represents the 118th unit. *B*: average force contributed by last-recruited motor units as a function of muscle force. Motor-unit force was expressed as a percentage of the overall muscle force developed during each trial. The relative increment in force due to recruitment declined hyperbolically with increased force (*B*) despite the linear relation between the twitch force of last-recruited units and muscle force (*A*).

force (De Luca 1985; De Luca et al. 1982). However, for the small forces (i.e., <50% maximum) associated with fine control, it would seem that this type of recruitment strategy may decrease the ability of a muscle to smoothly grade force. As discussed in a recent review (Kernell 1992) when excitation increases to a level just sufficient to activate a motor unit, the contribution of the unit to muscle force abruptly changes from zero to ~10–50% of the maximum force capacity of the unit. After recruitment, motor-unit force can then be continuously graded. Recruitment itself therefore represents a disruption in the process of smooth force gradation. Compression of the recruitment range into the low force region increases the magnitude of the recruitment-associated additions in force relative to the total force. This effect was illustrated in Fig. 12*B*, where the increment in force, relative to the total force, due to recruitment was larger in the narrow recruitment range condition. Dispersing recruitment over a large force range therefore effectively decreases the magnitude of the recruitment-related force steps relative to the total force.

A consistent empirical result for motor units in several muscles has been the observation of a nearly linear relationship between twitch force of a motor unit and the muscle force at which the unit was recruited (Calancie and Bawa 1985; Goldberg and Derfler 1977; Milner-Brown et al. 1973b; Monster and Chan 1977; Riek and Bawa 1992; Stephens and Usherwood 1977; Thomas et al. 1987; Yemm 1977; Zajac and Faden 1985). On the basis of this finding, it has been pointed out that this kind organization offers a built-in control over muscle force because the relative increment in force associated with recruitment should remain nearly constant over a large force range (Harrison 1983; Henneman and Olson 1965; Kernell 1992; Milner-Brown et al. 1973b; Zajac and Faden 1985). However, as was shown in Fig. 12, the existence of a linear relationship between twitch force and recruitment threshold did not translate into a constant increment in force due to recruitment. The slower contractile speed of low-threshold motor units caused them to respond to the threshold firing rate with greater relative force output as compared with that produced by later-recruited, fast-contracting units. Consequently, these simulations suggested that constancy in the relative force contributed by newly recruited units is an unlikely organizational property of motor-unit pools.

It is important to point out that experimental work in human muscles such as first dorsal interosseus has indicated that recruitment may be complete before 50% of maximum force (De Luca et al. 1982; Milner-Brown et al. 1973b). It is possible, however, that the actual upper limit of recruitment may be higher but has not been observed because of technical limitations. Detection of recruitment onsets becomes increasingly difficult with increased force, because activity in other units contaminate the myoelectric signal used to discriminate single-unit behavior. The exploration of recruitment behavior in motor units therefore has generally been restricted to submaximal force levels. Until new methodologies become available that provide the capacity to reliably monitor the complete functional range in large samples of motor units, the prediction of a broad recruitment range by the model is difficult to validate. Moreover, the limited empirical information currently available

regarding motor-unit behavior at high force levels represents a major impediment to a complete understanding of how motor-unit pools are organized.

Maximum force

None of the conditions tested yielded the maximum force capacity of the simulated muscle. At maximum excitation for the condition shown in Fig. 6, the PFRs of the lowest and highest threshold units were, respectively, 35 and 25 imp/s, and the mean rate for the entire pool was 31.6 imp/s, a value comparable with and perhaps slightly higher than that found experimentally (26.4 imp/s, Bigland-Ritchie et al. 1983; 28.2 imp/s, Bigland-Ritchie et al. 1992). The force produced for this condition, however, was only 77% of the calculated maximum force capacity of the muscle. This deficit in force output occurred in part because many of the large force units were firing at rates below that required for complete tetanus. However, when the peak firing rates were matched to the stimulus rates required for maximum force for each unit (Fig. 10), the force at maximum excitation was still less than the maximum capacity. This effect was attributed to the natural variability in ISIs, which, when superimposed on a nonlinear force-frequency curve, would tend to diminish the average force from what would be exerted if units discharged with constant intervals (see Fig. 11). Nonetheless, the matched firing rate condition was more effective, in terms of motor-unit activity, for producing force. At maximum excitation, the matched firing rate condition (Fig. 10) generated more force (86 vs. 77% of maximum force capacity) with an overall lower mean firing rate (24 vs. 31.6 imp/s) than the condition shown in Fig. 6. The conditions that yielded the largest force were those depicted in Figs. 7, *B* and *D*, where the mean rate at maximum excitation was 51.6 imp/s and force achieved 97% of the maximum capacity. For these conditions, most of the units were firing at mean rates well above that required for maximum tetanic force with constant rate stimulation. The overall mean rate of the pool for these simulations (51.6 imp/s), however, was well above that generally observed during maximum voluntary contractions. The discrepancy between the firing rates required to attain the maximum force capacity and the rates observed during maximum voluntary contractions implies that the force exerted by muscle during maximum voluntary efforts is, under normal circumstances, less than the maximum capacity of the muscle (De Luca et al. 1982; Enoka and Fuglevand 1993; Schwindt 1973).

Nonlinear response of muscle to excitatory drive

It is not immediately clear how the relationship between EMG and force could be linear considering the number of nonlinear factors that affect EMG and force. Some of these nonlinearities include EMG signal cancellation due to temporal overlap of negative phases of some motor-unit action potentials with the positive phases of others (Bernstein 1967; Moore 1967); the sigmoid relation between motor-unit force and firing rate; the saturation in motor-unit firing rates; the simultaneous increases in recruitment and firing rate with increased excitation within the recruitment range and increased firing rate only outside the recruitment

range; and the nonlinear distributions of recruitment thresholds, twitch forces, and action-potential amplitudes across the motor-unit population. The overall effect of these factors was to cause the input-output relationships for surface EMG and for muscle force to be nonlinear (Figs. 6, B and C). However, these nonlinear relationships between excitation and EMG and between excitation and force had similar forms. Consequently, when EMG was plotted as a function of force, a linear relation was exhibited. Therefore the existence of a linear EMG-force relationship does not imply that muscle force or EMG behave linearly, rather, it simply indicates that the respective input-output properties have a similar shape (Milner-Brown and Stein 1975).

The sigmoid shape between excitation and muscle force (e.g., Fig. 6C) has been demonstrated previously (Heckman and Binder 1991) and has important implications for motor control. At small forces, the gain of the system is low. The low gain provides stable control over force in the force region where many fine motor tasks are performed. At higher forces, the gain of the muscle force system is augmented. Therefore large increases in force, such as that required in powerful muscular efforts, could be achieved through a moderate enhancement in muscle excitation. The plateau in force development at the highest force levels suggests that a substantial increase in synaptic excitation would be required to drive muscle force over the last 10–15% of its range. This plateau in the muscle force-excitation curve has been shown to occur even when motoneurons are simulated to discharge in the secondary, high-gain region of the firing rate-synaptic current relationship (Heckman and Binder 1991). The functional implication of the plateau is that it should become progressively more difficult, in a synaptic excitation sense, to effect an increase in force at high force levels.

In summary, a motor-unit pool model was developed to facilitate a quantitative examination of the relationships among neural input, muscle force, and the surface EMG. Comparison of simulated muscle output for various recruitment/rate coding schemes to empirical information was used to identify feasible structures of motor-unit systems. The utility of the population-based model was that the input to muscle was known exactly and could be readily manipulated. This allowed the exploration of some issues of motor-unit pool organization that would be difficult to examine experimentally.

The authors gratefully acknowledge the helpful comments of Dr. C. J. Heckman.

Address for reprint requests: A. J. Fuglevand, John B. Pierce Laboratory, 290 Congress Ave., New Haven, CT 06519.

Received 16 March 1993; accepted in final form 9 August 1993.

REFERENCES

- ANDREASSEN, S. AND ARENDT-NIELSEN, L. Muscle fibre conduction velocity in motor units of the human anterior tibial muscle: a new size principle parameter. *J. Physiol. Lond.* 391: 561–571, 1987.
- ANDREASSEN, S. AND ROSENFALCK, A. Regulation of the firing pattern of single motor units. *J. Neurol. Neurosurg. Psychiatry* 43: 897–906, 1980.
- ARMSTRONG, J. B., ROSE, P. K., VANNER, S., BAKKER, G. J., AND RICHMOND, F. J. R. Compartmentalization of motor units in the cat neck muscle, biventer cervicis. *J. Neurophysiol.* 60: 31–44, 1988.
- BAWA, P. AND STEIN, R. B. Frequency response of human soleus muscle. *J. Neurophysiol.* 39: 788–793, 1976.
- BELLEMARE, F., WOODS, J. J., JOHANSSON, R., AND BIGLAND-RITCHIE, B. Motor-unit discharge rates in maximal voluntary contractions of three human muscles. *J. Neurophysiol.* 50: 1380–1392, 1983.
- BENDAT, J. S. AND PIERSOL, A. G. *Engineering Applications of Correlation and Spectral Analysis*. New York: Wiley-Interscience, 1980.
- BERNSHTEIN, V. M. Modeling the electrical signal of a group of muscle fibers. *Biofizika* 12: 1059–1063, 1967.
- BIGLAND, B. AND LIPPOLD, O. C. J. The relation between force, velocity and integrated electrical activity in human muscles. *J. Physiol. Lond.* 123: 214–224, 1954a.
- BIGLAND, B. AND LIPPOLD, O. C. J. Motor unit activity in the voluntary contraction of human muscle. *J. Physiol. Lond.* 125: 322–335, 1954b.
- BIGLAND-RITCHIE, B., FURBUSH, F. H., GANDEVIA, S. C., AND THOMAS, C. K. Voluntary discharge frequencies of human motoneurons at different muscle lengths. *Muscle Nerve* 15: 130–137, 1992.
- BIGLAND-RITCHIE, B., JOHANSSON, R., LIPPOLD, O. C. J., SMITH, S., AND WOODS, J. J. Changes in motoneurone firing rates during sustained maximal voluntary contractions. *J. Physiol. Lond.* 340: 335–346, 1983.
- BIGLAND-RITCHIE, B. AND WOODS, J. J. Changes in muscle contractile properties and neural control during human muscular fatigue. *Muscle Nerve* 7: 691–699, 1984.
- BINDER, M. D. AND MENDELL, L. M. (Editors). *The Segmental Motor System*. Oxford, UK: Oxford Univ. Press, 1990.
- BODINE, S. C., ROY, R. R., ELDRED, E., AND EDGERTON, V. R. Maximal force as a function of anatomical features of motor units in the cat tibialis anterior. *J. Neurophysiol.* 57: 1730–1745, 1987.
- BOTTERMAN, B. R., IWAMOTO, G. A., AND GONYEA, W. J. Gradation of isometric tension by different activation rates in motor units of cat flexor carpi radialis muscle. *J. Neurophysiol.* 56: 494–506, 1986.
- BROWNSTONE, R. M. *On Regulation of Repetitive Firing of Lumbar Motoneurons During Fictive Locomotion in the Cat* (PhD thesis). Winnipeg, Canada: Univ. of Manitoba, 1989.
- BUCHTHAL, F., GULD, C., AND ROSENFALCK, P. Propagation velocity in electrically activated muscle fibers in man. *Acta Physiol. Scand.* 34: 75–89, 1955.
- BUCHTHAL, F., GULD, C., AND ROSENFALCK, P. Multielectrode study of the territory of a motor unit. *Acta Physiol. Scand.* 39: 83–104, 1957.
- BUCHTHAL, F. AND SCHMALBRUCH, H. Contraction times and fibre types in intact human muscle. *Acta Physiol. Scand.* 79: 435–452, 1970.
- BURKE, R. E. Firing patterns of gastrocnemius motor units in the decerebrate cat. *J. Physiol. Lond.* 196: 631–654, 1968.
- BURKE, R. E. Motor units: anatomy, physiology, and functional organization. In: *Handbook of Physiology. The Nervous System. Motor Control*. Bethesda, MD: Am. Physiol. Soc., 1981, sect. 1, vol. II, part 1, p. 345–422.
- BURKE, R. E., RUDOMIN, P., AND ZAJAC, F. E. Catch property in single mammalian motor units. *Science Wash. DC* 168: 122–124, 1970.
- BURKE, R. E., RUDOMIN, P., AND ZAJAC, F. E. The effect of activation history on tension production by individual muscle units. *Brain Res.* 109: 515–529, 1976.
- BURKE, R. E. AND TSAIRIS, P. Anatomy and innervation ratios in motor units of cat gastrocnemius. *J. Physiol. Lond.* 234: 749–765, 1973.
- CALANCIE, B. AND BAWA, P. Voluntary and reflexive recruitment of flexor carpi radialis motor units in humans. *J. Neurophysiol.* 53: 1194–1200, 1985.
- CALVIN, W. H. AND STEVENS, C. F. Synaptic noise and other sources of randomness in motoneuron interspike intervals. *J. Neurophysiol.* 31: 574–587, 1968.
- CHAMBERLAIN, S. AND LEWIS, D. W. Contractile characteristics and innervation ratio of rat soleus motor units. *J. Physiol. Lond.* 412: 1–21, 1989.
- CLAMANN, H. P. Statistical analysis of motor unit firing patterns in a human skeletal muscle. *Biophys. J.* 9: 1233–1251, 1969.
- CLAMANN, H. P. AND SCHELHORN, T. B. Nonlinear force addition of newly recruited motor units in the cat hindlimb. *Muscle Nerve* 11: 1079–1089, 1988.
- CORDO, P. J. AND RYMER, W. Z. Motor-unit activation patterns in lengthening and isometric contractions of hindlimb extensor muscles in the decerebrate cat. *J. Neurophysiol.* 47: 782–796, 1982.
- DAITA, A. K. AND STEPHENS, J. A. Synchronization of motor unit activity during voluntary contraction in man. *J. Physiol. Lond.* 422: 397–419, 1990.
- DE LUCA, C. J. Physiology and mathematics of myoelectric signals. *IEEE Trans. Biomed. Eng.* 26: 313–325, 1979.

- DE LUCA, C. J. Control properties of motor units. *J. Exp. Biol.* 115: 125–136, 1985.
- DE LUCA, C. J., LEFEVER, R. S., MCCUE, M. P., AND XENAKIS, A. P. Behavior of human motor units in different muscles during linearly varying contractions. *J. Physiol. Lond.* 329: 113–128, 1982.
- ENOKA, R. M. AND FUGLEVAND, A. J. Neuromuscular basis of the maximum force capacity of muscle. In: *Current Issues in Biomechanics*, edited by M. Grabiner. Champaign, IL: Human Kinetics, 1993, p. 215–235.
- FLESHMAN, J. W., MUNSON, J. B., AND SYPERT, G. W. Homonymous projection of individual group Ia-fibers to physiologically characterized medial gastrocnemius motoneurons in the cat. *J. Neurophysiol.* 46: 1339–1348, 1981a.
- FLESHMAN, J. W., MUNSON, J. B., SYPERT, G. W., AND FRIEDMAN, W. A. Rheobase, input resistance and motor-unit type in medial gastrocnemius motoneurons in the cat. *J. Neurophysiol.* 46: 1326–1338, 1981b.
- FREUND, H.-J., BÜDINGEN, H. J., AND DIETZ, V. Activity of single motor units from human forearm muscles during voluntary isometric contractions. *J. Neurophysiol.* 38: 933–946, 1975.
- FUGLEVAND, A. J. *A Motor Unit Pool Model: Relationship of Neural Control Properties to Isometric Muscle Tension and the Electromyogram* (PhD thesis). Waterloo, Canada: Univ. of Waterloo, 1989.
- FUGLEVAND, A. J., WINTER, D. A., PATLA, A. E., AND STASHUK, D. Motor unit recruitment and rate coding influences on muscle tension and EMG. *Soc. Neurosci. Abstr.* 15: 523, 1989.
- FUGLEVAND, A. J., WINTER, D. A., PATLA, A. E., AND STASHUK, D. Detection of motor unit action potentials with surface electrodes: influence of electrode size and spacing. *Biol. Cybern.* 67: 143–153, 1992.
- GOLDBERG, L. J. AND DERFLER, B. Relationship among recruitment order, spike amplitude, and twitch tension of single motor units in human masseter. *J. Neurophysiol.* 40: 879–890, 1977.
- GRANIT, R. Neuromuscular interaction in postural tone of the cat's isometric soleus muscle. *J. Physiol. Lond.* 143: 387–402, 1958.
- GRANIT, R., KERNELL, D., AND LAMARRE, Y. Algebraical summation in synaptic activation of motoneurons firing within the 'primary range' to injected currents. *J. Physiol. Lond.* 187: 379–399, 1966.
- GUSTAFSSON, B. AND PINTER, M. J. An investigation of threshold properties among cat spinal α-motoneurons. *J. Physiol. Lond.* 357: 453–483, 1984.
- GYDIKOV, A. AND KOSAROV, D. Some features of different motor units in human biceps brachii. *Pfluegers Arch.* 347: 75–88, 1974.
- HARRISON, P. J. The relationship between the distribution of motor unit mechanical properties and the forces due to recruitment and to rate coding for the generation of muscle force. *Brain Res.* 264: 311–315, 1983.
- HARRISON, P. J. AND TAYLOR, A. Individual excitatory post-synaptic potentials due to muscle spindle Ia afferents in cat triceps surae motoneurons. *J. Physiol. Lond.* 312: 455–470, 1981.
- HECKMAN, C. J. AND BINDER, M. D. Analysis of effective synaptic currents generated by homonymous Ia afferent fibers in motoneurons of the cat. *J. Neurophysiol.* 60: 1946–1966, 1988.
- HECKMAN, C. J. AND BINDER, M. D. Neural mechanisms underlying the orderly recruitment of motoneurons. In: *The Segmental Motor System*, edited by M. D. Binder and L. M. Mendell. Oxford, UK: Oxford Univ. Press, 1990, p. 182–204.
- HECKMAN, C. J. AND BINDER, M. D. Computer simulation of the steady-state input-output function of the cat medial gastrocnemius motoneuron pool. *J. Neurophysiol.* 65: 952–967, 1991.
- HENNEMAN, E. Relation between size of neurons and their susceptibility to discharge. *Science Wash. DC* 126: 1345–1347, 1957.
- HENNEMAN, E. Functional organization of motoneuron pools: the size-principle. In: *Integration in the Nervous System*, edited by H. Asunuma and V. J. Wilson. Tokyo: Igaku Shoin, 1979, p. 13–25.
- HENNEMAN, E. AND MENDELL, L. M. Functional organization of motoneuron pool and its inputs. In: *Handbook of Physiology. The Nervous System. Motor Control*. Bethesda, MD: Am. Physiol. Soc., 1981, sect. 1, vol. II, part 1, p. 423–507.
- HENNEMAN, E. AND OLSON, C. B. Relations between structure and function in the design of skeletal muscle. *J. Neurophysiol.* 28: 581–598, 1965.
- HENNEMAN, E., SOMJEN, G., AND CARPENTER, D. O. Functional significance of cell size in spinal motoneurons. *J. Neurophysiol.* 28: 560–580, 1965a.
- HENNEMAN, E., SOMJEN, G., AND CARPENTER, D. O. Excitability and inhibitory properties of motoneurons of different sizes. *J. Neurophysiol.* 28: 599–620, 1965b.
- HOFFER, J. A., SUGANO, N., LOEB, G. E., MARKS, W. B., O'DONOVAN, M. J., AND PRATT, C. A. Cat hindlimb motoneurons during locomotion. II. Normal activity patterns. *J. Neurophysiol.* 57: 530–553, 1987.
- JAMI, L. AND PETIT, R. Correlation between axonal conduction velocity and tetanic tension of motor units in four muscles of the cat hind limb. *Brain Res.* 96: 114–118, 1977.
- JOHNSON, M. A., POLGAR, J., WEIGHTMAN, D., AND APPLETON, D. Data on the distribution of fibre types in thirty-six human muscles: an autopsy study. *J. Neurol. Sci.* 18: 111–129, 1973.
- KANDA, K. AND HASHIZUME, K. Factors causing difference in force output among motor units in the rat medial gastrocnemius muscle. *J. Physiol. Lond.* 448: 677–695, 1992.
- KERNELL, D. The adaptation and the relation between discharge frequency and current strength of cat lumbosacral motoneurons stimulated by long-lasting injected currents. *Acta Physiol. Scand.* 65: 65–73, 1965a.
- KERNELL, D. High-frequency repetitive firing of cat lumbosacral motoneurons stimulated by long-lasting injected currents. *Acta Physiol. Scand.* 65: 74–86, 1965b.
- KERNELL, D. The limits of firing frequency in cat lumbosacral motoneurons possessing different time course of afterhyperpolarization. *Acta Physiol. Scand.* 65: 87–100, 1965c.
- KERNELL, D. Rhythmic properties of motoneurons innervating muscle fibres of different speed in m. gastrocnemius medialis of the cat. *Brain Res.* 160: 159–162, 1979.
- KERNELL, D. Organized variability in the neuromuscular system: a survey of task-related adaptations. *Arch. Ital. Biol.* 130: 19–66, 1992.
- KERNELL, D., EERBEEK, O., AND VERHEY, B. A. Motor unit categorization on basis of contractile properties: an experimental analysis of the composition of the cat's m. peroneus longus. *Exp. Brain Res.* 50: 211–219, 1983a.
- KERNELL, D., EERBEEK, O., AND VERHEY, B. A. Relation between isometric force and stimulation rate in cat's hindlimb motor units of different twitch contraction time. *Exp. Brain Res.* 50: 220–227, 1983b.
- KERNELL, D. AND MONSTER, A. W. Threshold current for repetitive impulse firing in motoneurons innervating muscle fibres of different fatigue sensitivity in the cat. *Brain Res.* 229: 193–196, 1981.
- KOMI, P. V. AND BUSKIRK, E. R. Effect of eccentric and concentric muscle conditioning on tension and electrical activity of human muscle. *Ergonomics* 15: 417–434, 1972.
- KUKULKA, C. G. AND CLAMANN, H. P. Comparison of the recruitment and discharge properties of motor units in human brachial biceps and adductor pollicis during isometric contractions. *Brain Res.* 219: 45–55, 1981.
- LAWRENCE, J. H. AND DE LUCA, C. J. Myoelectric signal versus force relationship in different human muscles. *J. Appl. Physiol.* 54: 1653–1659, 1983.
- LEXELL, J., DOWNHAM, D., AND SJÖSTRÖM, M. Distribution of different fibre types in human skeletal muscle. Fiber type arrangement in m. vastus lateralis from three groups of healthy men between 15 and 83 years. *J. Neurol. Sci.* 72: 211–222, 1986.
- LEXELL, J., TAYLOR, C. C., AND SJÖSTRÖM, M. What is the cause of ageing atrophy? Total number, size and proportion of different fiber types studied in whole vastus lateralis muscle from 15- to 83-year-old men. *J. Neurol. Sci.* 84: 275–294, 1988.
- LINDSAY, A. D. AND BINDER, M. D. Distribution of effective synaptic currents underlying recurrent inhibition in cat triceps surae motoneurons. *J. Neurophysiol.* 65: 168–177, 1991.
- MANNARD, A. AND STEIN, R. B. Determination of the frequency response of isometric soleus muscle in the cat using random nerve stimulation. *J. Physiol. Lond.* 229: 275–296, 1973.
- McDONAGH, J. C., BINDER, M. D., REINKING, R. M., AND STUART, D. G. A commentary on muscle unit properties in cat hindlimb muscles. *J. Morphol.* 166: 217–230, 1980.
- MC PHEDRAN, A. M., WUERKER, R. B., AND HENNEMAN, E. Properties of motor units in a homogenous red muscle (soleus) of the cat. *J. Neurophysiol.* 28: 71–84, 1965.
- MELLAH, S., RISPAL-PADEL, L., AND RIVIERE, G. Changes in excitability of motor units during preparation for movement. *Exp. Brain Res.* 82: 178–186, 1990.
- MENDELL, L. M. AND HENNEMAN, E. Terminals of single Ia fibers: loca-

- tion, density and distribution within a pool of 300 homonymous motoneurons. *J. Neurophysiol.* 34: 171–187, 1971.
- MILNER-BROWN, H. S. AND STEIN, R. B. The relation between the surface electromyogram and muscular force. *J. Physiol. Lond.* 246: 549–569, 1975.
- MILNER-BROWN, H. S., STEIN, R. B., AND YEMM, R. The contractile properties of human motor units during voluntary isometric contraction. *J. Physiol. Lond.* 228: 285–306, 1973a.
- MILNER-BROWN, H. S., STEIN, R. B., AND YEMM, R. The orderly recruitment of human motor units during voluntary isometric contractions. *J. Physiol. Lond.* 230: 359–370, 1973b.
- MILNER-BROWN, H. S., STEIN, R. B., AND YEMM, R. Changes in firing rate of human motor units during linearly changing voluntary contractions. *J. Physiol. Lond.* 230: 371–390, 1973c.
- MONSTER, A. W. AND CHAN, H. Isometric force production by motor units of extensor digitorum communis muscle in man. *J. Neurophysiol.* 40: 1432–1443, 1977.
- MOORE, A. D. Synthesized EMG waves and their implications. *Am. J. Phys. Med.* 46: 1302–1316, 1967.
- MOUNIER, Y., HOLY, X., AND STEVENS, L. Compared properties of the contractile system of skinned slow and fast rat muscle fibres. *Pfluegers Arch.* 415: 136–141, 1989.
- MUNSON, J. B. Synaptic inputs to type-identified motor units. In: *The Segmental Motor System*, edited by M. D. Binder and L. M. Mendell. New York: Oxford Univ. Press, 1990, p. 291–307.
- MUNSON, J. B., FLESHMAN, J. W., ZENGEL, J. E., AND SYPERT, G. W. Synaptic and mechanical coupling between type-identified motor units and individual spindle afferents of medial gastrocnemius muscle of the cat. *J. Neurophysiol.* 51: 1268–1283, 1984.
- MUNSON, J. B., SYPERT, G. W., ZENGEL, J. E., LOFTON, S. A., AND FLESHMAN, J. W. Monosynaptic projections of individual spindle group II afferents to type-identified medial gastrocnemius motoneurons in the cat. *J. Neurophysiol.* 48: 1164–1174, 1982.
- NORDSTROM, M. A., FUGLEVAND, A. J., AND ENOKA, R. M. Estimating the strength of common input to human motoneurons from the cross-correlogram. *J. Physiol. Lond.* 453: 547–574, 1992.
- NORDSTROM, M. A. AND MILES, T. A. Discharge variability and physiological properties of human masseter motor units. *Brain Res.* 541: 50–56, 1991.
- OLSON, C. B. AND SWETT, C. P. A functional and histochemical characterization of motor units in a heterogeneous muscle (flexor digitorum longus) of the cat. *Comp. Neurol.* 128: 475–498, 1966.
- PERSON, R. S. AND LIBKIND, M. S. Simulation of electromyograms showing interference patterns. *Electroencephalogr. Clin. Neurophysiol.* 28: 625–632, 1970.
- POWERS, R. K. AND BINDER, M. D. Distribution of oligosynaptic group I input to the cat medial gastrocnemius motoneuron pool. *J. Neurophysiol.* 53: 497–517, 1985.
- RACK, P. M. H. AND WESTBURY, D. R. The effects of length and stimulus rate on tension in the isometric cat soleus muscle. *J. Physiol. Lond.* 204: 443–460, 1969.
- RIEK, S. AND BAWA, P. Recruitment of motor units in human forearm extensors. *J. Neurophysiol.* 68: 100–108, 1992.
- SALTIN, B. AND GOLLNICK, P. D. Skeletal muscle adaptability: significance for metabolism and performance. In: *Handbook of Physiology. Skeletal Muscle*. Bethesda, MD: Am. Physiol. Soc., 1983, sect. 10, p. 555–631.
- SCHWINDT, P. C. Membrane potential trajectories underlying motonuron rhythmic firing at high rates. *J. Neurophysiol.* 36: 434–449, 1973.
- SCHWINDT, P. C. AND CRILL, W. E. Membrane properties of cat spinal motoneurons. In: *Handbook of the Spinal Cord. Anatomy and Physiology*, edited by R. A. Pandolf. New York: Dekker, 1984, vols. 2 and 3, p. 199–242.
- SOLOMONOW, M., ZHOU, B.-H., BARATTA, R., SHOJI, H., AND D'AMBROSIA, R. EMG-force relationships of a skeletal muscle as a function of recruitment range. *IEEE 8th Annu. Conf. Eng. Med. Biol. Soc.*, 1986, p. 500–502.
- STÅLBERG, F. Propagation velocity in human muscle fibers in situ. *Acta Physiol. Scand. Suppl.* 70: 1–112, 1966.
- STÅLBERG, E. AND ANTONI, L. Electrophysiological cross section of the motor unit. *J. Neurol. Neurosurg. Psychiatry* 43: 469–474, 1980.
- STÅLBERG, E. AND THIELE, B. Discharge pattern of motoneurones in humans. In: *New Developments in Electromyography and Clinical Neurophysiology*, edited by J. E. Desmedt. Basel: Karger, 1973, vol. 3, p. 234–241.
- STEIN, R. B., FRENCH, A. S., MANNARD, A., AND YEMM, R. New methods for analysing motor function in man and animals. *Brain Res.* 40: 187–192, 1972.
- STEIN, R. B. AND PARMIGIANI, F. Nonlinear summation of contractions in cat muscles. I. Early depression. *J. Gen. Physiol.* 78: 277–293, 1981.
- STEPHENS, J. A. AND USHERWOOD, T. P. The mechanical properties of human motor units with special reference to their fatigability and recruitment threshold. *Brain Res.* 125: 91–97, 1977.
- STUART, D. G. AND ENOKA, R. M. Motoneurons, motor units, and the size principle. In: *The Clinical Neurosciences. Neurobiology*, edited by R. N. Rosenberg and W. D. Willis. New York: Churchill Livingstone, 1983, sect. 5, p. 471–517.
- SYPERT, G. W., FLESHMAN, J. W., AND MUNSON, J. B. Comparison of monosynaptic actions of medial gastrocnemius group Ia and group II muscle spindle afferents on triceps surae motoneurons. *J. Neurophysiol.* 44: 726–738, 1980.
- TANJI, J. AND KATO, M. Firing rate of individual motor units in voluntary contraction of abductor digiti minimi muscle in man. *Exp. Neurol.* 40: 771–783, 1973.
- TAYLOR, A. The significance of grouping of motor unit activity. *J. Physiol. Lond.* 162: 259–269, 1962.
- THOMAS, C. K., BIGLAND-RITCHIE, B., AND JOHANSSON, R. S. Force-frequency relationships of human thenar motor units. *J. Neurophysiol.* 65: 1509–1516, 1991.
- THOMAS, C. K., JOHANSSON, R. S., WESTLING, G., BIGLAND-RITCHIE, B. Twitch properties of human thenar motor units measure in response to intraneuronal motor-axon stimulation. *J. Neurophysiol.* 64: 1339–1346, 1990.
- THOMAS, C. K., ROSS, B. H., AND CALANCIE, B. Human motor-unit recruitment during isometric contractions and repeated dynamic movements. *J. Neurophysiol.* 57: 311–324, 1987.
- TÖTÖSY DE ZEPETNEK, J. E., ZUNG, H. V., ERDEBIL, S., AND GORDON, T. Innervation ratio is an important determinant of force in normal and reinnervated rat tibialis anterior muscles. *J. Neurophysiol.* 67: 1385–1403, 1992.
- VREDENBREGT, J. AND RAU, G. Surface electromyography in relation to force, muscle length, and endurance. In: *New Developments in Electromyography and Clinical Neurophysiology*, edited by J. E. Desmedt. Basel: Karger, 1973, p. 607–622.
- WINTER, D. A. *Biomechanics of Human Movement*. New York: Wiley, 1979.
- WOODS, J. J. AND BIGLAND-RITCHIE, B. Linear and non-linear surface EMG-force relationships in human muscle. *Am. J. Phys. Med.* 62: 287–299, 1983.
- WUERKER, R. B., MCPHEDRAN, A. M., AND HENNEMAN, E. Properties of motor units in a heterogeneous pale muscle (m. gastrocnemius) of the cat. *J. Neurophysiol.* 28: 85–99, 1965.
- YELLIN, H. A histochemical study of muscle spindles and their relationship to extrafusal fiber types in the rat. *Am. J. Anat.* 125: 31–46, 1969.
- YEMM, R. The orderly recruitment of motor units of the masseter and temporal muscles during voluntary isometric contractions in man. *J. Physiol. Lond.* 265: 163–174, 1977.
- YOUNG, J. L. AND MAYER, R. F. Physiological properties and classification of single motor units activated by intramuscular microstimulation in the first dorsal interosseous in man. In: *Motor Unit Types, Recruitment, and Plasticity in Health and Disease. Progress in Clinical Neurophysiology*, edited by J. E. Desmedt. Basel: Karger, 1981, vol. 9, p. 17–25.
- ZAJAC, F. E. AND FADEN, J. S. Relationship among recruitment order, axonal conduction velocity, and muscle-unit properties of type-identified motor units in cat plantaris muscle. *J. Neurophysiol.* 53: 1303–1322, 1985.
- ZENGEL, J. E., REID, S. A., SYPERT, G. W., AND MUNSON, J. B. Membrane electrical properties and prediction of motor-unit type of medial gastrocnemius motoneurons in the cat. *J. Neurophysiol.* 53: 1323–1344, 1985.